

NASA CONTRACTOR  
REPORT

NASA CR - 61017

NASA CR - 61017

FACILITY FORM 802	N 65 12336 (ACCESSION NUMBER)	_____ (THRU)
	88 (PAGES)	1 (CODE)
	CR 61017 (NASA CR OR TMX OR AD NUMBER)	11 (CATEGORY)

APOLLO LOGISTICS SUPPORT SYSTEMS MOLAB STUDIES REPORT  
T. V. SYSTEMS STUDIES FOR A  
LUNAR MOBILE LABORATORY

Prepared under Contract No. NAS85307 by

J. C. McBride

HAYES INTERNATIONAL CORPORATION  
Missile and Space Support Division  
Apollo Logistics Support Group

GPO PRICE \$ \_\_\_\_\_

OTS PRICE(S) \$ \_\_\_\_\_

Hard copy (HC) 3.00

Microfiche (MF) .75

For

NASA - GEORGE C. MARSHALL SPACE FLIGHT CENTER  
Huntsville, Alabama

October 1964

APOLLO LOGISTICS SUPPORT SYSTEMS MOLAB STUDIES REPORT  
T. V. SYSTEMS STUDIES FOR A  
LUNAR MOBILE LABORATORY

by

J. C. McBride

Prepared under Contract No. NAS8-5307 by

HAYES INTERNATIONAL CORPORATION

Missile and Space Support Division

Apollo Logistics Support Group

For

ASTRIONICS LABORATORY

This report is reproduced photographically  
from copy supplied by the contractor.

NASA-GEORGE C. MARSHALL SPACE FLIGHT CENTER

NOTICE

This report was prepared as an account of Government sponsored work. Neither the United States, nor the National Aeronautics and Space Administration (NASA), nor any person acting on behalf of NASA:

- A.) Makes any warranty or representation, expressed or implied, with respect to the accuracy, completeness, or usefulness of the information contained in this report, or that the use of any information, apparatus, method, or process disclosed in this report may not infringe privately owned rights; or
- B) Assumes any liabilities with respect to the use of, or for damages resulting from the use of any information, apparatus, method or process disclosed in this report.

As used above, "person acting on behalf of NASA" includes any employee or contractor of NASA, or employee of such contractor, to the extent that such employee or contractor of NASA, or employee of such contractor prepares, disseminates, or provides access to, any information pursuant to his employment or contract with NASA, or his employment with such contractor.

Requests for copies of this report should be referred to

National Aeronautics and Space Administration  
Office of Scientific and Technical Information  
Attention: AFSS-A  
Washington, D.C. 20546

TABLE OF CONTENTS

<u>Section</u>	<u>Title</u>	<u>Page</u>
1.0	LUNAR PHOTOMETRY . . . . .	1
1.1	Introduction . . . . .	1
1.2	Illumination . . . . .	1
1.2.1	Direct Sunlight . . . . .	3
1.2.2	Earthshine . . . . .	3
1.2.3	Starlight . . . . .	6
1.3	Albedos . . . . .	6
1.4	Photometric Function . . . . .	8
1.4.1	Description . . . . .	8
1.4.2	Use During Direct Sunlight . . . . .	12
1.4.3	Use During Earthshine . . . . .	16
1.5	Brightness . . . . .	16
2.0	OPTICS AND SCANNING REQUIREMENTS . . . . .	24
2.1	Resolution of Objects . . . . .	24
2.2	Optics and Resolution . . . . .	26
2.3	Lens Photometry . . . . .	34
2.4	Aperture and Shutter Control . . . . .	40
3.0	BANDWIDTH CONSIDERATIONS . . . . .	41
3.1	Bandwidth Equations . . . . .	41
3.2	Frame Rate Versus Vehicle Velocity . . . . .	42
3.3	Resolution Ratio . . . . .	46
3.4	Graphs . . . . .	46

TABLE OF CONTENTS (CONT)

<u>Section</u>	<u>Title</u>	<u>Page</u>
3.5	Stereoptics . . . . .	51
3.6	Range Finding . . . . .	52
3.7	Bandwidth Reduction . . . . .	57
4.0	ARTIFICIAL ILLUMINATION . . . . .	59
4.1	Photocathode Illumination . . . . .	59
4.2	Spectral Response Considerations . . . . .	65
5.0	UP-LINK TELEVISION SUB-SYSTEM . . . . .	69
5.1	Requirements . . . . .	69
5.2	Scanning Parameters and Bandwidth . . . . .	69
5.3	Power Levels and Receiver Quality . . . . .	70
5.4	Monitor . . . . .	72
REFERENCES	. . . . .	74

## LIST OF ILLUSTRATIONS

<u>Figure</u>	<u>Title</u>	<u>Page</u>
1-1	Illumination Sources During Lunation . . . . .	2
1-2	Brightness of Center Point . . . . .	10
1-3	Photometric Function . . . . .	11
1-4	$\alpha$ and $\varphi$ . . . . .	13
1-5	Angle of Incidence . . . . .	13
1-6	$\gamma$ and h . . . . .	14
1-7	$\varphi$ Positive . . . . .	15
1-8	Geometry for Plot of Brightness . . . . .	18
1-9	Example 1 - Plot of Brightness . . . . .	19
1-10	Example 2 - Brightness Variation . . . . .	23
2-1	Resolution of Objects . . . . .	25
2-2	Optical Parameters . . . . .	27
2-3	1" Vid 500 = $N_R$ . . . . .	30
2-4	2" Vid 500 = $N_R$ . . . . .	31
2-5	1" Vid 650 = $N_R$ . . . . .	32
2-6	Focal Length Versus Lines of Resolution . . . . .	33
2-7	Lens Photometry . . . . .	35
2-8	Photocathode Illumination vs Brightness . . . . .	38
3-1	Video Signal . . . . .	42
3-2	Delay Times in Control Loop . . . . .	43
3-3	Scan Converter Block Diagram . . . . .	45

LIST OF ILLUSTRATIONS (CONT)

<u>Figure</u>	<u>Title</u>	<u>Page</u>
3-4	Bandwidth Chart . . . . .	47
3-5	Bandwidth Chart . . . . .	48
3-6	Bandwidth Chart . . . . .	49
3-7	Bandwidth Chart . . . . .	50
3-8	Range Finder Geometry . . . . .	54
3-9	Range Finder Error Graph . . . . .	56
4-1	Solid Angle of Conical Section . . . . .	60
4-2	P.C. Illumination vs Distance Artificial Illumination . . . . .	64
4-3	Spectral Response Curves . . . . .	68

LIST OF TABLES

<u>Table</u>	<u>Title</u>	<u>Page</u>
1-I	Direct Solar Illumination . . . . .	3
1-II	Table of Albedos of Typical Lunar Areas . . . . .	7
1-III	Variation in Angles, Example 1 . . . . .	20
1-IV	Variation in Angles, Example 2 . . . . .	22
2-I	Vertical Raster Sizes . . . . .	26
4-I	Efficiencies of Possible Sources . . . . .	62



# LIST OF SYMBOLS

## SYMBOLS - SECTION 1.0

$\Theta$  Phase angle of moon  $0^\circ$  at aphelion (full moon)

$\beta$  Selenographic latitude + for north

$\lambda$  Selenographic longitude + for east

$\alpha$  Angle measured between line of incidence and line of emittance measured in the slant plane

$i$  Angle of incidence to a plane, measured from the normal to that plane

$\epsilon$  Angle of emittance measured from the normal to the plane

$\tau$  Auxiliary angle measured in the slant plane from line of emittance to projection of normal in the slant plane

Slant Plane - described by the line of incidence and the line of emittance

$h$  Heading angle of the MOLAB, measured from north

$\gamma$  The angle measured between the normal planes containing the line of incidence and the local meridian

$L$  Longitudinal libration

SYMBOLS - SECTION 2.0

s	Object distance
s'	Image distance
d	Vertical field of view
d'	Raster height
$\sigma$	Minimum resolvable height of object
$\sigma'$	Minimum resolvable image
N <sub>a</sub>	Number of active scanning lines
h	Height of camera or optical objective
F	f/number
f	Focal length
f <sub>v</sub>	Vertical frame rate
N	Numbers of scanning lines
N <sub>r</sub>	Number of lines of resolution
w	Horizontal field of view
$\delta$	Minimum resolvable width of object
$\Theta_v$	Vertical viewing angle

## 1.0 LUNAR PHOTOMETRY

### 1.1 INTRODUCTION

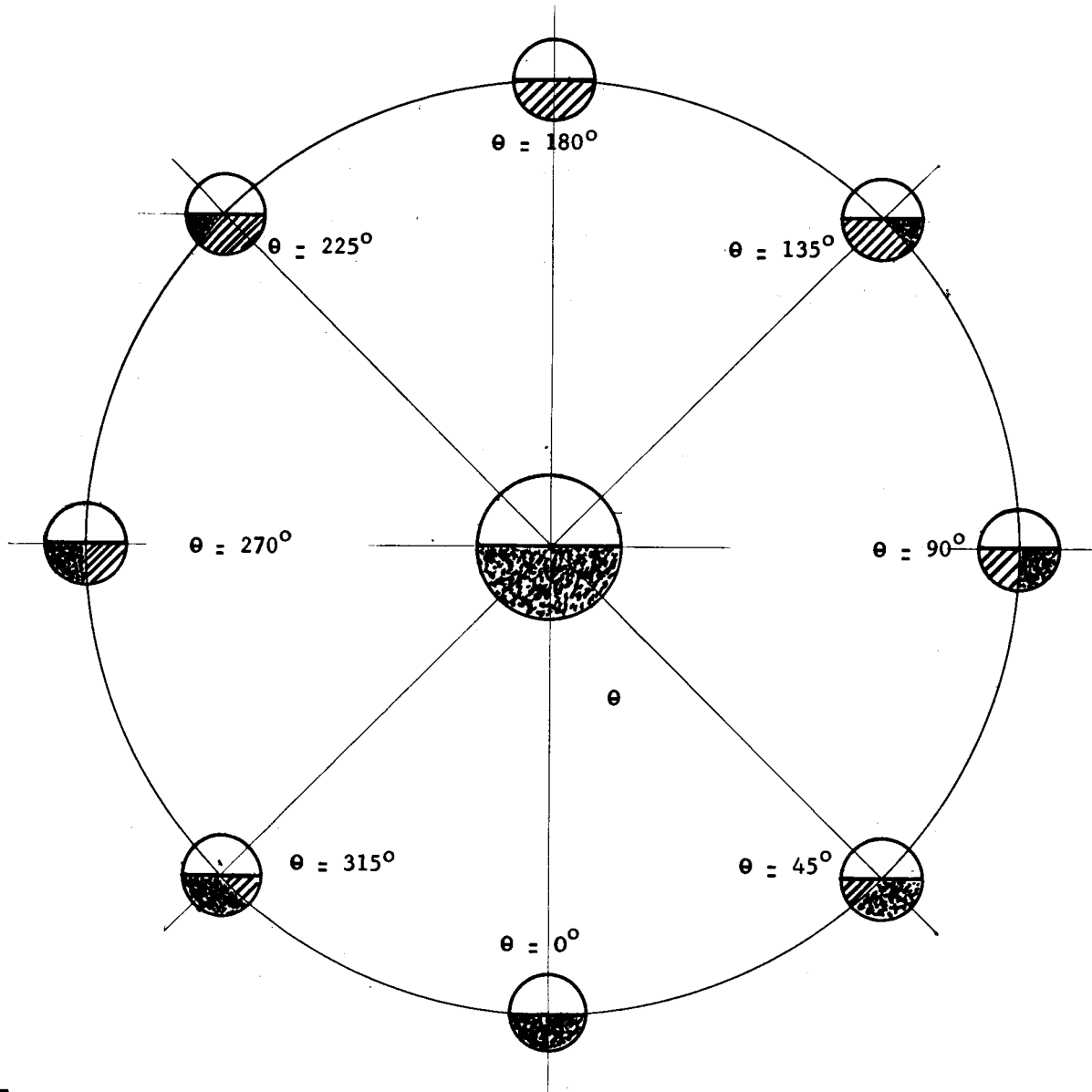
The available surface brightness of the moon must first be considered, in order to determine the requirements of the optics and television pick-up device to be used aboard the Lunar Mobile Laboratory. This brightness will be a function of the illumination level (either direct sunlight or earthshine), the albedo of the lunar surface, and a dimensionless photometric function. The photometric function relates the brightness to the angles of incidence and emittance, as well as their relative positions.


### 1.2 ILLUMINATION

Figure 1-1 shows the position of the moon with respect to the earth and sun during a complete lunation. The moon is shown sectioned into direct sunlight areas, earthshine areas, and non-illuminated areas. The visible half of the moon receives some degree of illumination during the complete lunation; however, it is marginal at the limb areas during certain phases.

The angle  $\Theta$  is used to describe the phase of the moon and is taken to be  $0^\circ$  at full moon. Because of the ellipticity of the lunar orbit,  $\Theta$  is not a simple function of time but can be determined as  $\Theta = 12.2 D + L$ , where  $D$  is days since full moon and  $L$  is the longitudinal libration which has limits of plus or minus  $6.5^\circ$ .

SOLAR IRRADIATION



 Earth Shine

 Sunshine

$$\frac{d\theta}{dt} = 0.508 \text{ degrees/hr.}$$

FIGURE 1-1 ILLUMINATION SOURCES DURING LUNATION



absence of direct sunlight due to the relative magnitudes of the two. A possible exception to this is at the terminator when the sunlight approaches zero.

The illumination due to the earthshine is a function of: (1) the time of the year, (2) the earth's albedo, and, (3) the earth-moon distance. The time of the year determines the available solar illumination on the earth. The proper value can be extracted from Table 1-I.

The albedo of the earth ranges from 0.32 to 0.52 with a mean value of 0.36. The value depends on the amount of cloud cover present and, to a lesser extent, that portion of the earth reflecting the light, i.e., the percent of land - water.

The illuminated area of the earth as seen from the moon varies with the phase angle  $\Theta$ . At full earth,  $\Theta = 180^\circ$ , the area is that of the full earth disk, and decreases to half that value at 1st or 3rd quarter. An equation for this area is the sum of 1/2 disk and an area of 1/2 an ellipse whose semi-minor axis is  $R_e \cos (\Theta - 180^\circ)$

$$A_e = \frac{\pi R_e^2}{2} + \frac{\pi R_e}{2} \left[ R_e \cos (\Theta - 180^\circ) \right] \quad (1-2)$$

$$A_e = \frac{\pi R_e^2}{2} \left[ 1 + \cos (\Theta - 180^\circ) \right] \quad (1-3)$$

There is no limitation on  $\Theta$ , and the  $(1 + \cos \Theta - 180^\circ)$  term is 2 when  $\Theta = 180^\circ$  (full earth) and 0 when  $\Theta = 0^\circ$  (new earth).

The intensity of the earth considered as a source is the brightness per square unit times the area.

The brightness is determined by  $B_E = \frac{E_s \rho_e}{\pi}$  (1-4)

where  $E_s$  is the luminous solar constant and  $\rho_e$  is the earth's albedo.

If  $E_s$  is lumens/m<sup>2</sup>, then  $B_E$  will be in candles/m<sup>2</sup>.

The illumination due to earthshine will then be:

$$E = \frac{I}{d^2} = \frac{B_E \cdot A_e}{d^2} \quad (1-5)$$

substituting for  $A_e$  and  $B_E$

$$E_{ES} = \frac{E_s \rho_e \cdot \frac{\pi R_e^2}{2} [1 + \cos (\Theta - 180^\circ)]}{d^2} \quad (1-6)$$

$$E_{ES} = \frac{E_s \rho_e R_e^2 [1 + \cos (\Theta - 180^\circ)]}{2 d^2} \quad (1-7)$$

where  $E_s$  = solar illumination at sun-earth distance

$\rho_e$  = earth albedo

$R_e$  = radius of earth

$d$  = earth moon distance

$\Theta$  = lunar phase angle

$E_{ES}$  = illumination due to earthshine:

Using a minimum  $E_s$ , a maximum value for  $d$ , and a  $\rho_e = 0.36$ , the illumination at a  $\Theta = 90^\circ$  or  $270^\circ$  is 6.54 lux. This can be considered a minimum value during that period when earthshine is the primary source of illumination.

An equation based on mean values throughout becomes:

$$E_{ES} = 7.58 [1 + \cos (\Theta - 180^\circ)] \text{ lux} \quad (1-8)$$

The illumination at full earth ( $\odot - 180^\circ$ ) is  $2 \times 7.58 = 15.15$  lux and at 1st or 3rd quarter ( $\odot = 90^\circ$  or  $270^\circ$ ), is 7.58 lux.

### 1.2.3 STARLIGHT

A third source of illumination will be starlight, which will have a value of  $2.2 \times 10^{-3}$  lux.<sup>6</sup> This amount of illumination can be significant only under the worst possible conditions of earthshine, i.e., extreme angles of incidence and emittance.

### 1.3 ALBEDOS

In Table I-II, a list of albedos and the range of variation is supplied for reference. The table is taken from Reference 6, which is a compilation of values listed at the bottom of the table.

The albedo is defined as the Normal Albedo - the ratio of luminance of the lunar surface when observed as parallel to the illuminating rays to the luminance of a Lambert surface of unit reflectivity. The term "luminance" dictates the response of the eye as the reference and cannot be considered exact for the camera response.

The albedos were determined by observation here on earth and must be considered as mean values of an area determined by the physical constants (aperture) of the telescope used. The camera on the lunar surface will, of course, be viewing a much smaller area which could have an albedo vastly different from the value given in the table.





Where it is a factor in the graphs or equations, an albedo of 0.07 will be used.

Although it is said that there is little color on the moon, the albedo is not constant throughout the entire spectrum of solar radiation. For example, Markov<sup>10</sup> states "the surroundings of Copernicus are characterized by relatively large absorption of ultra-violet rays. The actual rays of the system of Copernicus reflect relatively few ultra-violet rays, while the spaces between them reflect relatively many. The same occurs for Kepler". An increased contrast ratio, therefore, could be expected in the ultra-violet region. In the final analysis, this varying albedo due to wavelength should be considered when making the choice of spectral sensitivity of the camera tube.

#### 1.4 PHOTOMETRIC FUNCTION

##### 1.4.1 DESCRIPTION

A multiple series of quantitative brightness measurements were made by Fedoret's Sytinskya and Sharonov. Fedoret's data consisted of 41 points taken at 40 phases and the curves were derived from the data. For a graphic illustration, see Parker<sup>5</sup>, pages 35-65. From these observations, the following conclusions were reached:

- a) When observing the full moon from the earth, the brightness is maximum and is only a function of the albedo of the particular point. Under this condition, the angle of incidence is varying (a function of selenographic longitude and latitude), but the difference angle between incidence and

emittance is zero.

- b) If the center of the visible disk ( $0^\circ$  selenographic longitude and latitude) is observed during a complete lunation, the brightness will vary according to the curves of Figure 1-2. In this plot the angle of incidence equals the phase angle, while the angle of emittance is zero.
- c) Finally, if many points of the lunar surface are observed during the lunation, a family of curves is determined. Figure 1-3 is a deviation of these curves, using a change in parameter. Under these conditions, the angle of incidence is taken as the algebraic sum of phase angle  $\Theta$  and the selenographic longitude  $\lambda$ . The angle of emittance is equal to the longitude since the point of observation is earth. The observations show that the isophots (lines of equal brightness) follow the meridians so that the function is not dependent on the latitude. This again assumes that the effects of albedo are accounted for and the point of observation is earth.

In NASA Project Apollo Working Paper No. 1100, this same data of Fedoret is presented in terms of two auxiliary angles  $\alpha$  and  $\mathcal{T}$  that are functions of incidence, emittance, and the spherical angle measured between them so that the value of  $\theta$  can be determined under conditions other than observation from earth.

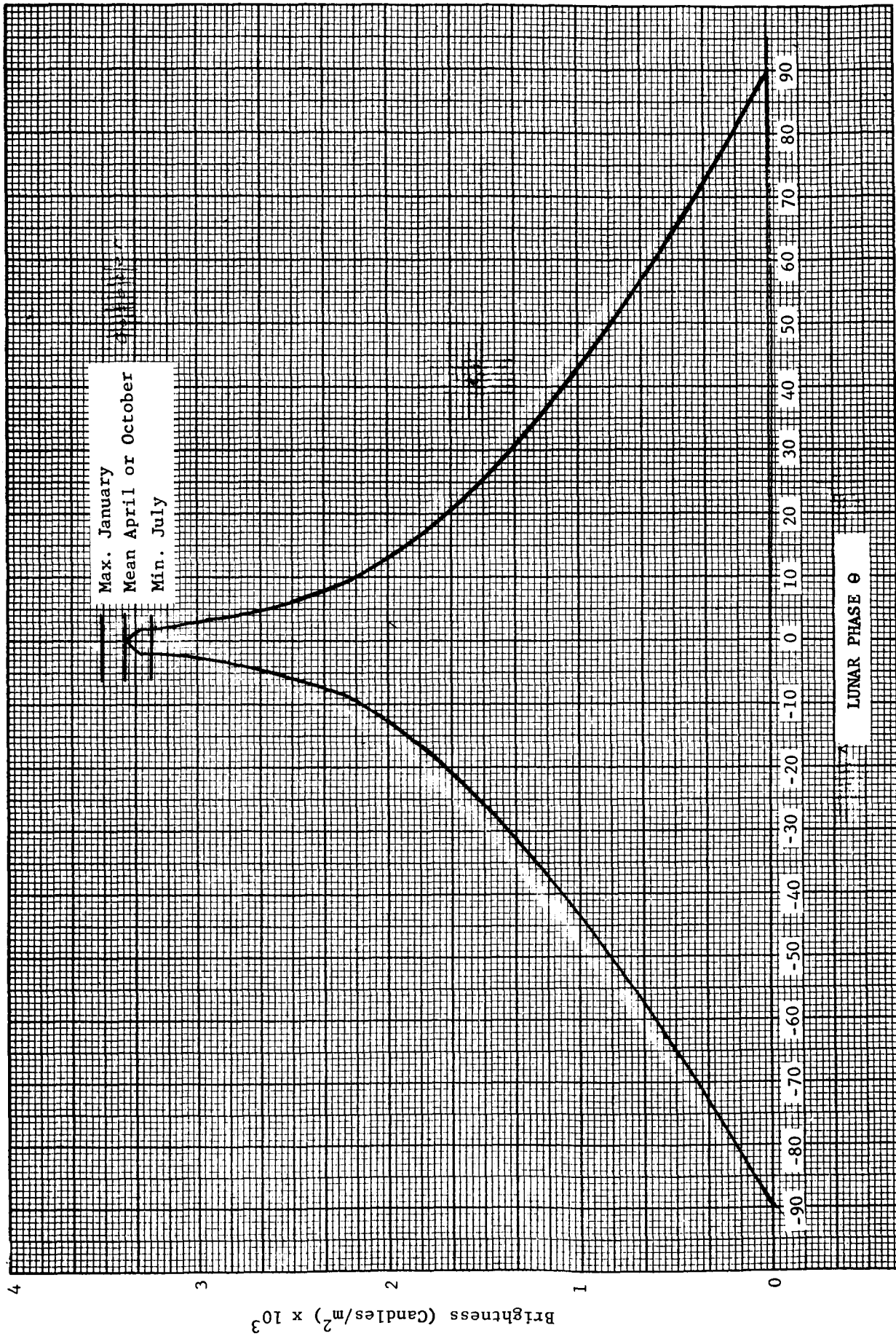


FIGURE 1-2 BRIGHTNESS OF CENTER POINT

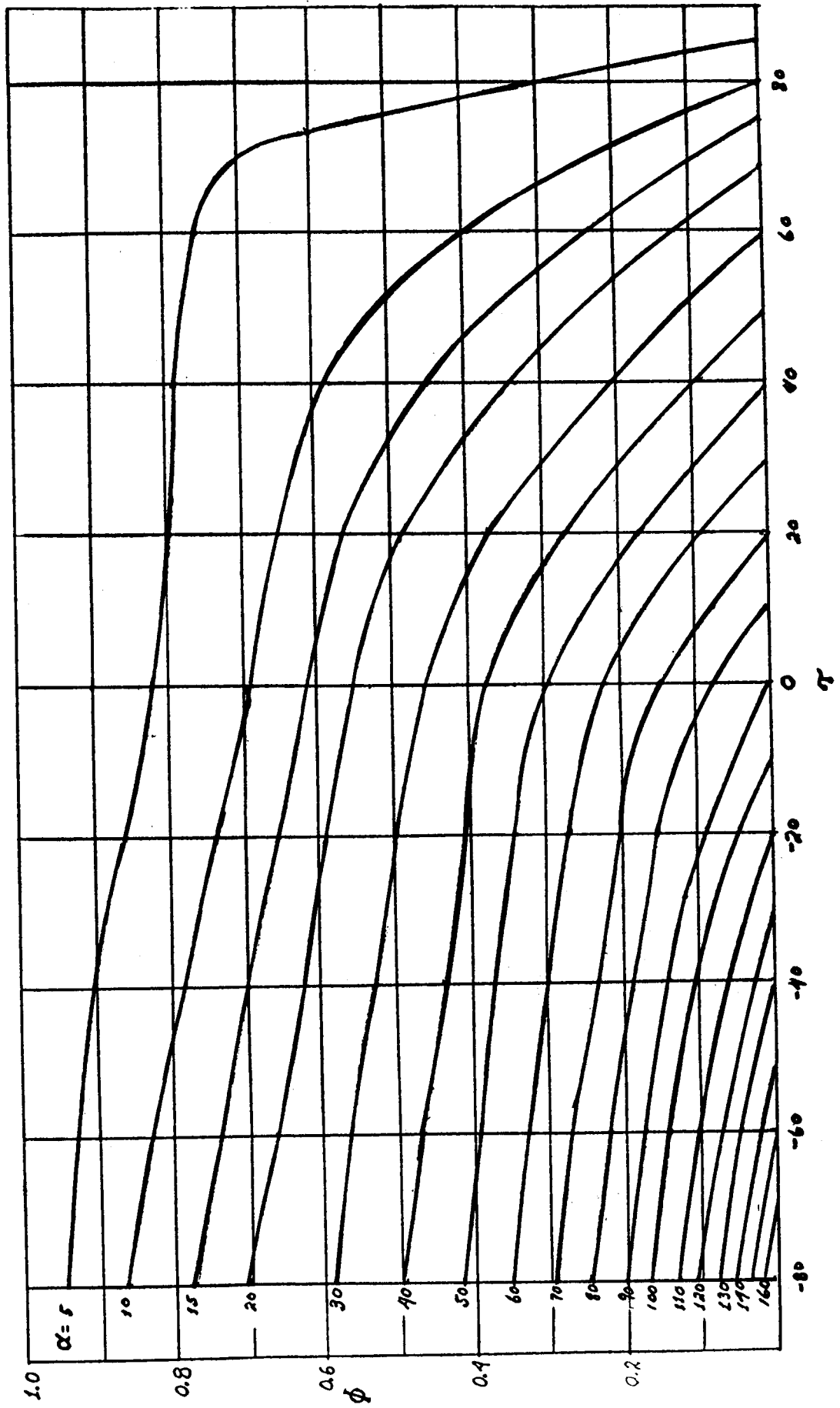


FIGURE 1-3 PHOTOMETRIC FUNCTION

Figure 1-4 shows the geometry in determining  $\alpha$  and  $\tau$ .  $\alpha$  is the third side of an oblique spherical triangle whose other two sides are  $i$  and  $\epsilon$ . The angle  $\tau$  is the projection of  $\epsilon$  into the slant plane (a plane determined by the lines of incidence and emittance).  $\tau$  can be shown as the angle between the line of emittance and the projection of the normal into the slant plane.

Then, for a given value of  $\alpha$  and  $\tau$ , the corresponding value of the photometric function  $\phi$  can be found from Figure 1-3, which then will be used to complete the solution for the surface brightness.

#### 1.4.2 USE DURING DIRECT SUNLIGHT

In order to relate the alpha-tau diagram to that of the lunar phase angle and selenographic coordinates, the angle of incidence must first be determined. Figure 1-5 shows the moon  $\odot$  degrees after full moon. The point P is shown at positive longitude  $\lambda$  (east) and positive latitude (north) in relation to the sub-earth point E. The angle of incidence is then the solution of the right spherical triangle whose other two sides are: the latitude  $\beta$  and the algebraic sum of the phase angle  $\odot$ , and the longitude  $\lambda$ . This solution is:

$$i = \arccos [\cos \beta \cos (\odot - \lambda)] \quad (1-9)$$

The sign of  $\beta$  can be included since the cosine function is positive in both the first and third quadrants. However  $(\odot - \lambda)$  must be limited to  $\pm 90^\circ$  to keep the point P in the direct sunlight area.

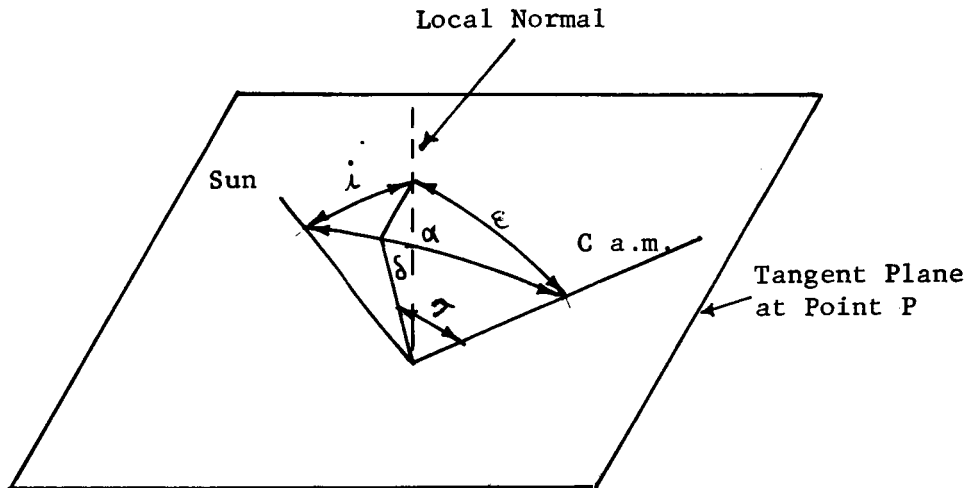


FIGURE 1-4  $\alpha$  AND  $\gamma$

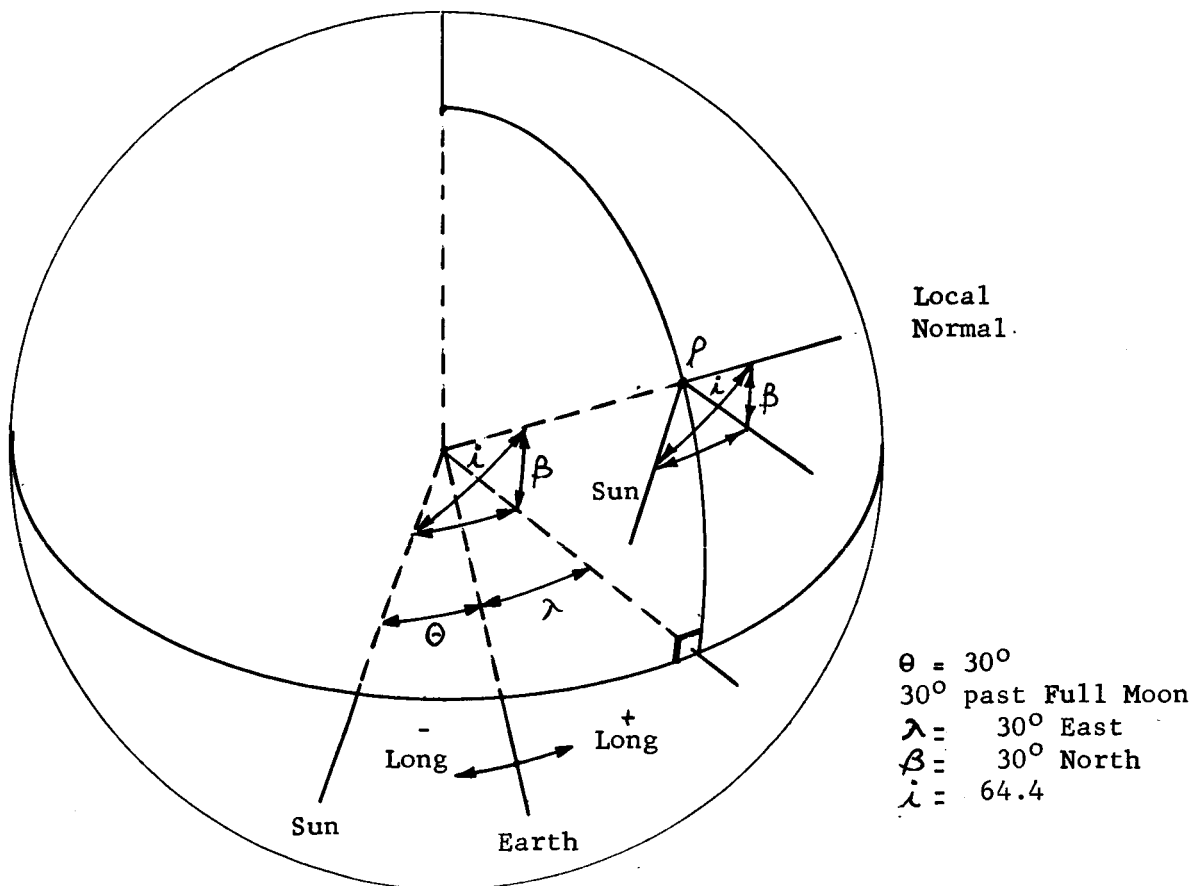


FIGURE 1-5 ANGLE OF INCIDENCE

Notice that if the point P is on the equator ( $\beta = 0$ ), then  $i$  equals  $(\theta - \lambda)$ .

Before  $\alpha$  can be determined, an auxiliary angle  $\gamma$  must be solved.  $\gamma$  is the angle included by the sides  $i$  and  $\beta$ , and the solution is:

$$\gamma = \text{arc cos} \left[ \tan \beta \cot i \right] \quad (1-10)$$

Figure 1-6 shows a normal view of the point P. The intersection of the two projections is the normal to the tangent plane at point P.  $\gamma$  is the angle between the projection of the line of incidence and the meridian passing through point P. The heading of the MOIAB is now introduced as  $h$ . The angle between the lines is  $\gamma - h$ . This angle will be used in the solution of  $\alpha$  and  $\tau$ . Using Figure 1-4, the solution for  $\alpha$  is that of an oblique spherical triangle where  $\alpha$  is the third side and the other two sides are  $i$  and  $\epsilon$ , with the included angle between them  $\gamma - h$ . Using the law of cosines,

$$\alpha = \text{arc cos} \left[ \cos i \cos \epsilon - \sin i \sin \epsilon \cos (\gamma - h) \right] \quad (1-11)$$

Notice that if  $(\gamma - h) = 0^\circ$ , then  $\alpha$  becomes  $i - \epsilon$  or if either  $i$  or  $\epsilon$  equals 0,  $\alpha$  becomes equal to the other.

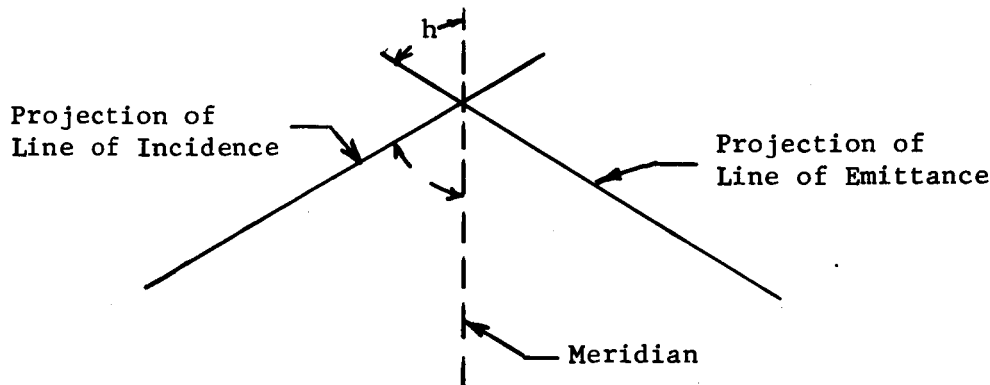


FIGURE 1-6  $\gamma$  AND  $h$



The second auxiliary angle  $\mathcal{T}$ , used in determining  $\theta$ , can be found by dividing the oblique spherical triangle into two right spherical triangles as in Figure 1-4. The angle  $\delta$  is the angle between the normal and the projection of the normal. Then both triangles are solved by:

$$\cos i = \cos (\alpha - \mathcal{T}) \cos \delta \quad (1-12)$$

$$\cos \varepsilon = \cos \mathcal{T} \cos \delta \quad (1-13)$$

By substituting the second equation in the first and expanding the cosine of the difference of two angles:

$$\cos i = \left[ \cos \alpha \cos \mathcal{T} + \sin \alpha \sin \mathcal{T} \right] \frac{\cos \varepsilon}{\cos \mathcal{T}} \quad (1-14)$$

Simplying and solving for  $\mathcal{T}$ :

$$\mathcal{T} = \arctan \frac{\cos i - \cos \alpha \cos \varepsilon}{\sin \alpha \cos \varepsilon} \quad (1-15)$$

The sign of tau will be negative in almost all cases for the MOLAB problem. Figure 1-7 shows the peculiar case when tau becomes positive. Here the source is below the line of emittance  $i > \varepsilon$  and  $\alpha$  is small. The projection falls outside of the  $i$ - $\varepsilon$ - $\alpha$  oblique triangle:

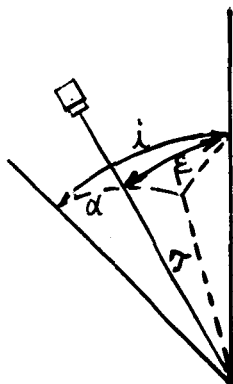


FIGURE 1-7  $\mathcal{T}$  POSITIVE

In all other cases, tau is taken to be negative.

### 1.4.3 USE DURING EARTHSHINE

When the source of illumination is earthshine, the angle of incidence is no longer a function of the phase angle  $\Theta$ . In section 1.4.2, the equation for  $i$  will still be true if  $\Theta$  is held at 0. The angle of incidence on the lunar surface will be:

$$i = \text{arc cos} [\cos \beta \cos \lambda] \quad (1-16)$$

Although the angle of incidence is not a function of  $\Theta$ , the amount of illumination definitely is, therefore, the brightness will be determined by the  $\Theta$  angle during both direct sunlight and earthshine, but for different reasons.

### 1.5 BRIGHTNESS

Once the amount of illumination has been determined, the albedo value has been chosen, and the photometric function has been taken, then the surface brightness can be computed from:

$$B = \frac{E \rho}{\pi} \phi \quad (1-17)$$

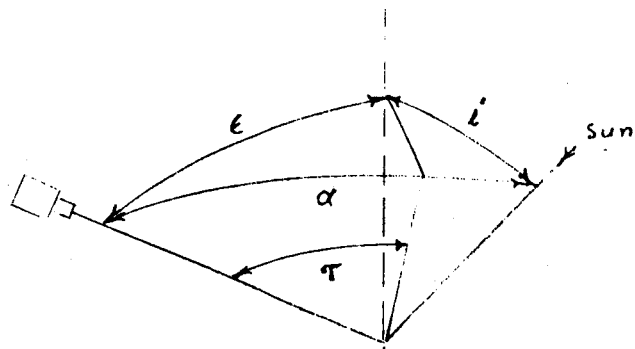
$P$  and  $\phi$  are dimensionless and the dimensions for  $B$  will be determined by those used for  $E$ . If  $E$  is lux (lumens/m<sup>2</sup>) then  $B$  will be in candles/m<sup>2</sup>.

E is either taken from Table 1-I, when direct sunlight is involved ( $-90 \leq \Theta \leq +90$ ), or computed from equation 1-7, when earthshine is the source ( $+90 \leq \Theta \leq 270$ ). The value of  $\rho$  to be used can be taken from Table 1-II and used directly. The value of  $\phi$  can be found by:

- a) Determining  $i$  from  $\Theta, \lambda, \beta$  in equation (1-9)
- b) Determining  $\gamma$  from  $\beta, i$  in equation (1-10)
- c) Determining  $\alpha$  from  $i, e, \gamma, h$  in equation (1-11)  
 $\epsilon$  and  $h$  will be direct functions of the MOLAB heading and camera tilt.
- d) Determining  $\tau$  from  $i, \alpha, \epsilon$ ; equation (1-15)
- f) Using Figure 1-3, selecting  $\alpha$  curve and finding  $\tau$  along the abscissa, then  $\phi$  at the intersection.

The first example of a brightness variation is taken at a fixed point midway between the Copernicus - Kelper regions or approximately  $\beta = +10^\circ$  North latitude and  $\lambda = -30^\circ$  West longitude. The vehicle is continuously headed east ( $h = +90^\circ$ ) and the downward tilt of the camera is 20 degrees. The illumination used is the mean value of direct sunlight and the curve extends from sunrise ( $\Theta = -60$ ) to sunset ( $\Theta = +120$ ). This would correspond to 14.74 earth days. Figure 1-8 shows the geometry for three points of the lunar day. In the late afternoon, the alpha angle diminishes, causing the peak in brightness.

Table 1 - III is included to show the variation in the angles, and Figure 1-9 graphs the brightness during the sunlight period.



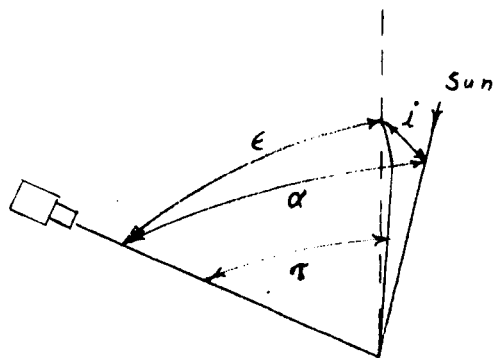
60° Before Noon

$$i = 60.5^\circ$$

$$\epsilon = 70.5^\circ$$

$$\alpha = 130.5^\circ$$

$$\tau = 70^\circ$$



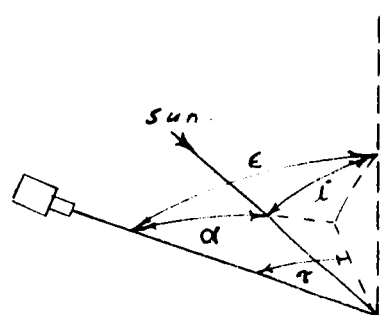
Noon

$$i = 10^\circ =$$

$$\epsilon = 70^\circ$$

$$\alpha = 70.2^\circ$$

$$\tau = -69.5^\circ$$



30° After Noon

$$i = 31.5^\circ$$

$$\epsilon = 70^\circ$$

$$\alpha = 41^\circ$$

$$\tau = -46^\circ$$

FIGURE 1-8 GEOMETRY FOR PLOT OF BRIGHTNESS

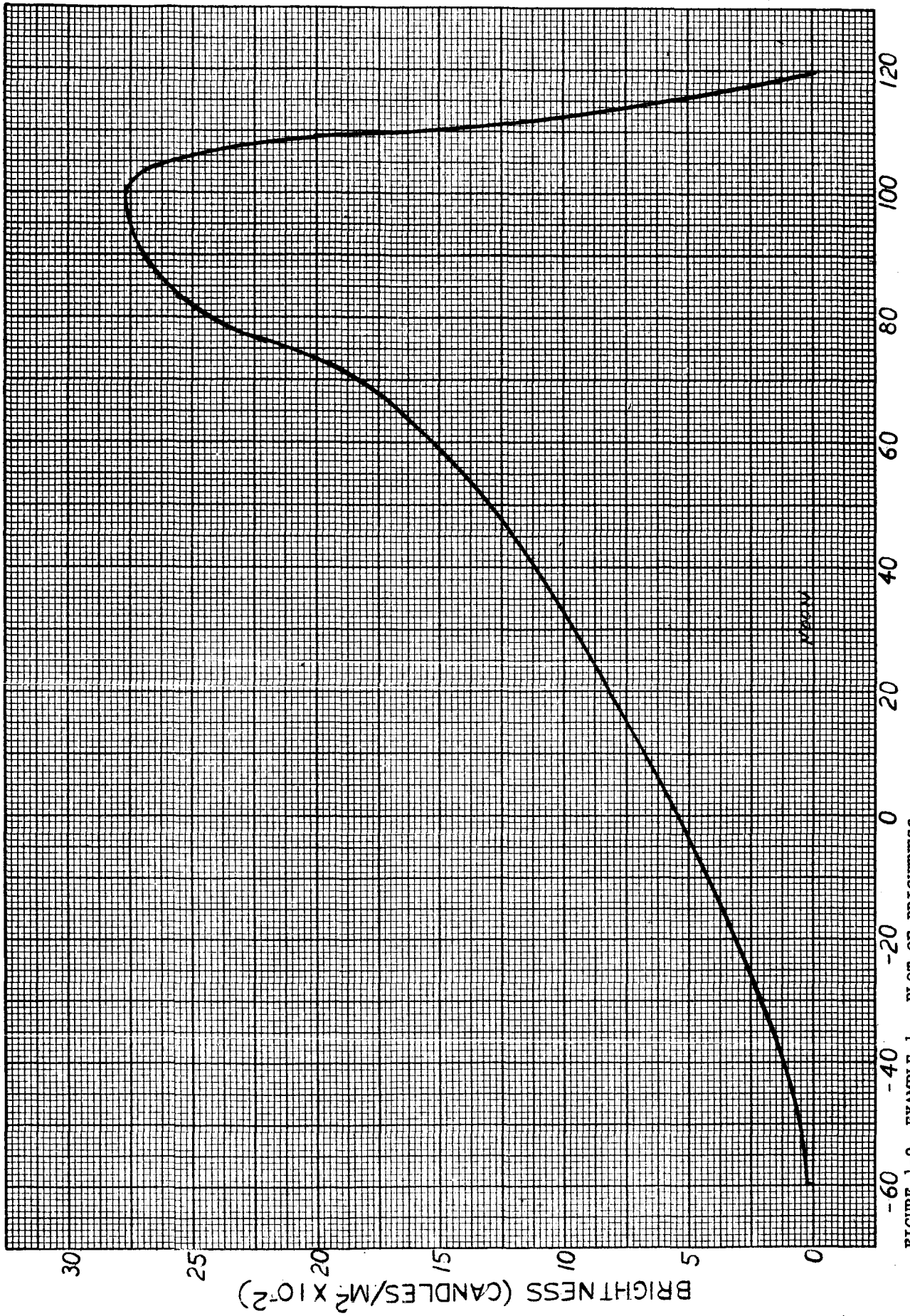


FIGURE 1-9 EXAMPLE 1 - PLOT OF BRIGHTNESS

TABLE 1 - III

VARIATION IN ANGLES, EXAMPLE 1								
	$\Theta =$	$i =$	$\gamma =$	$\gamma - h =$	$\alpha =$	$\alpha -$	$\phi =$	$\beta =$
Sunrise	-60	90	-90	-180	.160	-70°	0	0
	-30	60.5°	-84°	-174	130	-70	.06	202
	0	31.6	-73	-163.5	101°	-70°	.16	812
Noon	+30	+10	0	-90	70.2	-69.5°	.28	946
	+60	31.5	73°	-71°	41°	-46°	.45	1520
	+90	60.5°	84.2°	-6°	11°	-48°	.8	2700
	+100	70.3	86.3	-3.7	5.8	-70	.82	2760
Sunset	+120	90	90	0	20	-70°	.01	1950
								brightness
								candle/m <sup>2</sup>

The second example shows the vehicle at coordinates  $\beta = 20^\circ$  North and  $\lambda = 30^\circ$  West. The sun is  $60^\circ$  to the east or 118 earth hours before noon, at that longitude. Table 1 - IV shows a tabulation of the angles of interest and Figure 1-10 is a polar plot in the change in brightness as the vehicle rotates through  $360^\circ$ . The factor difference in this non-extreme example is 15.3:1. The brightness values were computed from the mean value of direct sunlight ( $15.15 \times 10^4$  lumens/ $m^2$ ), and an albedo of 7% was used. The tilt or depression angle of the camera was again  $20^\circ$ , which is somewhat greater than might normally be expected. A tilt of  $5^\circ$ , giving a emittance angle of  $85^\circ$ , would cause the curve to be lower in mean value, having a shorter duration peak toward the terminator.

The second example shows the vehicle at coordinates  $\beta = 20^\circ$  North and  $\lambda = 30^\circ$  West. The sun is  $60^\circ$  to the east or 118 earth hours before noon, at that longitude. Table 1 - IV shows a tabulation of the angles of interest and Figure 1-10 is a polar plot in the change in brightness as the vehicle rotates through  $360^\circ$ . The factor difference in this non-extreme example is 15.3:1. The brightness values were computed from the mean value of direct sunlight ( $15.15 \times 10^4$  lumens/ $m^2$ ), and an albedo of 7% was used. The tilt or depression angle of the camera was again  $20^\circ$ , which is somewhat greater than might normally be expected. A tilt of  $5^\circ$ , giving a emittance angle of  $85^\circ$ , would cause the curve to be lower in mean value, having a shorter duration peak toward the terminator.



The second example shows the vehicle at coordinates  $\beta = 20^\circ$  North and  $\lambda = 30^\circ$  West. The sun is  $60^\circ$  to the east or 118 earth hours before noon, at that longitude. Table 1 - IV shows a tabulation of the angles of interest and Figure 1-10 is a polar plot in the change in brightness as the vehicle rotates through  $360^\circ$ . The factor difference in this non-extreme example is 15.3:1. The brightness values were computed from the mean value of direct sunlight ( $15.15 \times 10^4$  lumens/ $m^2$ ), and an albedo of 7% was used. The tilt or depression angle of the camera was again  $20^\circ$ , which is somewhat greater than might normally be expected. A tilt of  $5^\circ$ , giving a emittance angle of  $85^\circ$ , would cause the curve to be lower in mean value, having a shorter duration peak toward the terminator.

The second example shows the vehicle at coordinates  $\beta = 20^\circ$  North and  $\lambda = 30^\circ$  West. The sun is  $60^\circ$  to the east or 118 earth hours before noon, at that longitude. Table 1 - IV shows a tabulation of the angles of interest and Figure 1-10 is a polar plot in the change in brightness as the vehicle rotates through  $360^\circ$ . The factor difference in this non-extreme example is 15.3:1. The brightness values were computed from the mean value of direct sunlight ( $15.15 \times 10^4$  lumens/ $m^2$ ), and an albedo of 7% was used. The tilt or depression angle of the camera was again  $20^\circ$ , which is somewhat greater than might normally be expected. A tilt of  $5^\circ$ , giving a emittance angle of  $85^\circ$ , would cause the curve to be lower in mean value, having a shorter duration peak toward the terminator.

TABLE 1 - IV

## VARIATION IN ANGLES, EXAMPLE 2

MOLAB located at  $\beta = + 20^\circ$   $\lambda = - 30^\circ$   $\theta = - 30$ Angle of incidence =  $62^\circ$   $\gamma = - 78.8^\circ$ 

Heading	$h$	$r-h$	$\alpha$	$\tau$	$\phi$	$\beta$
North	$0^\circ$	-78.8	71.1	-48	.25	846
North East	$45^\circ$	-123.8	107.5	-61	.11	372
East	90	-168.8	130.8	-70.5	.07	236
South East	135	147	121.7	-66	.08	270
South	180	101.2	90	-59	.18	610
South West	225	56.8	57	-44	.36	1215
West	270	11.2	12	-62.4	.83	2800
North West	315	33.8	32	-44.6	.52	1750
Max	-78.8	0	7.25	-70	.92	3105
Min	101.2	180	132	-70	.06	203

candles/m<sup>2</sup>

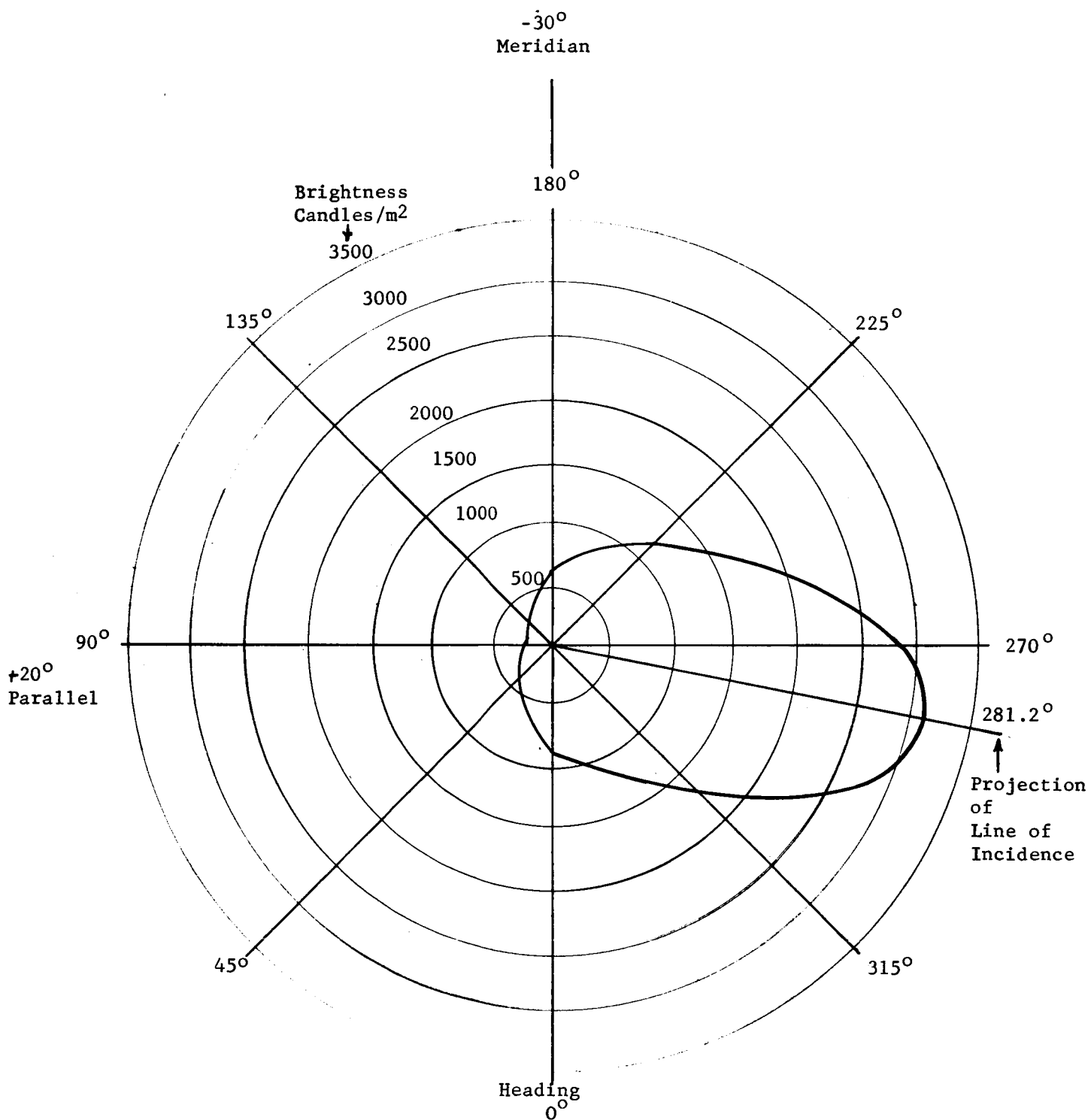


FIGURE 1-10 EXAMPLE 2 - BRIGHTNESS VARIATION  
23

## 2.0 OPTICS AND SCANNING REQUIREMENTS

### 2.1 RESOLUTION OF OBJECTS

Figure 2-1 shows two different types of objects to be resolved by a television camera at a distance  $s$  and mounted at a height  $h$ .

The top diagram shows a vertical object of height  $v$  and presents a resolved height  $\sigma$ , which subtends the angle  $\gamma$  at the camera lens. The depression angle of the camera is  $90^\circ - \theta$ . The value of  $\sigma$  can be found from:

$$\sigma = \sin \text{arc tan } \frac{s}{h} \quad (2-1)$$

and the value of  $\gamma$  from:

$$\gamma = \text{arc tan } \frac{dv}{h^2 + d^2 - vh} \quad (2-2)$$

If  $d$  is much greater than  $h$  or  $v$ , then the expression reduces to:

$$\gamma = \text{arc tan } \frac{v}{d} \quad (2-3)$$

For a 25 cm object at a distance of 100 meters and viewed from a height of 2 meters,  $\gamma = .142^\circ$  and  $\sigma = 25 \text{ cm } (24.995)$ .

The bottom diagram of Figure 2-1 shows the geometry for the similiar problem of a horizontal obstacle such as a crevice laying across the path of the vehicle. The subtended angle  $\gamma$  is:

$$\gamma = \text{arc tan } \frac{h v}{h^2 - s^2 - sv} \quad (2-4)$$

$$\frac{\delta}{v} = \sin \theta$$

$$\theta = \arcsin \tan' \frac{S}{h}$$

$$\delta = v \arcsin \tan \frac{S}{h}$$

$$\delta = \frac{S \cdot v}{S'}$$

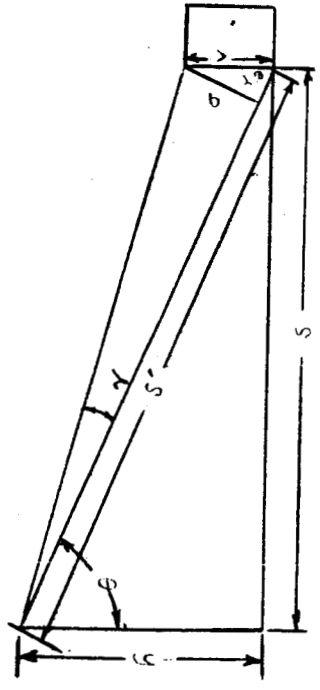
$$(S')^2 = S^2 + h^2$$

$$\gamma = \arcsin \tan \frac{\delta}{S' - \delta}$$

$$\frac{S \cdot v}{S'}$$

$$\gamma = \arcsin \tan \frac{\frac{S \cdot v}{S'}}{S' - \frac{S \cdot v}{S'}}$$

$$\gamma = \arcsin \tan \frac{S \cdot v}{S'^2 + h^2 - v \cdot h}$$



$$\frac{\delta}{v} = \cos \theta$$

$$\theta = \arcsin \tan \frac{S}{h}$$

$$\delta = v \arcsin \tan \frac{S}{h}$$

$$\delta = \frac{h \cdot v}{S'}$$

$$\gamma = \arcsin \tan \frac{\delta}{S' - \delta}$$

$$\gamma = \arcsin \tan \frac{\frac{h \cdot v}{S'}}{S' - \frac{h \cdot v}{S'}}$$

$$\gamma = \arcsin \tan \frac{h \cdot v}{S'^2 + S^2 - S \cdot v}$$

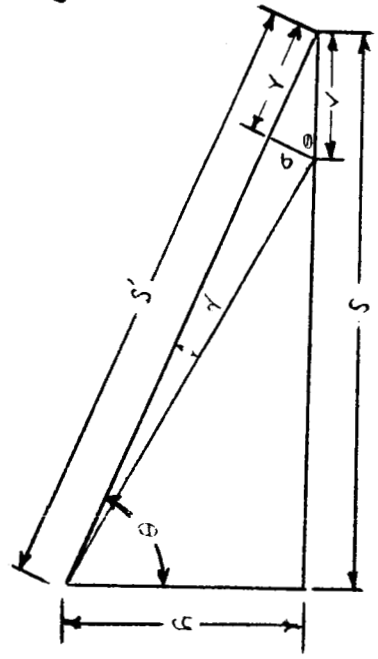


FIGURE 2-1

RESOLUTION OF OBJECTS

and the resolved object height is:

$$\sigma = v \cos \text{arc tan } \frac{s}{h} \quad (2-5)$$

For a 25 cm crevice, at a distance of 100 meters and a camera height of 2 meters,  $\sigma = .5$  cm (5mm) and  $\tau = .00288$  degrees (10.35 seconds of arc).

Of the two standard objects, the crevice presents a much more severe problem and if one considers that the nearer lip of the crevice could be higher than the far lip, or if the lighting angle was such that no shadow was cast, the problem becomes even greater.

## 2.2 OPTICS AND RESOLUTION

Knowing the vertical size of the minimum resolvable element  $\sigma$ , the balance between the camera's resolution and the optics producing the image can be determined. In Figure 2-2, the relation of the object, image, and lens is shown where  $d'$  is the height of the raster on the photocathode. Table 2-I lists several vidicons using a square or commercial type raster.  $Ud$  is the length of the diagonal of the useful area, and  $A$  is the aspect ratio width-to-height.

TABLE 2-I

VERTICAL RASTER SIZES

Tube Size	$Ud$	$A$	$d'$
1"	15.74 mm	1:1	11.12 mm
1"	15.74 mm	4:3	9.53 mm
2"	35.56 mm	1:1	25.15 mm
2"	35.56 mm	4:3	21.38 mm

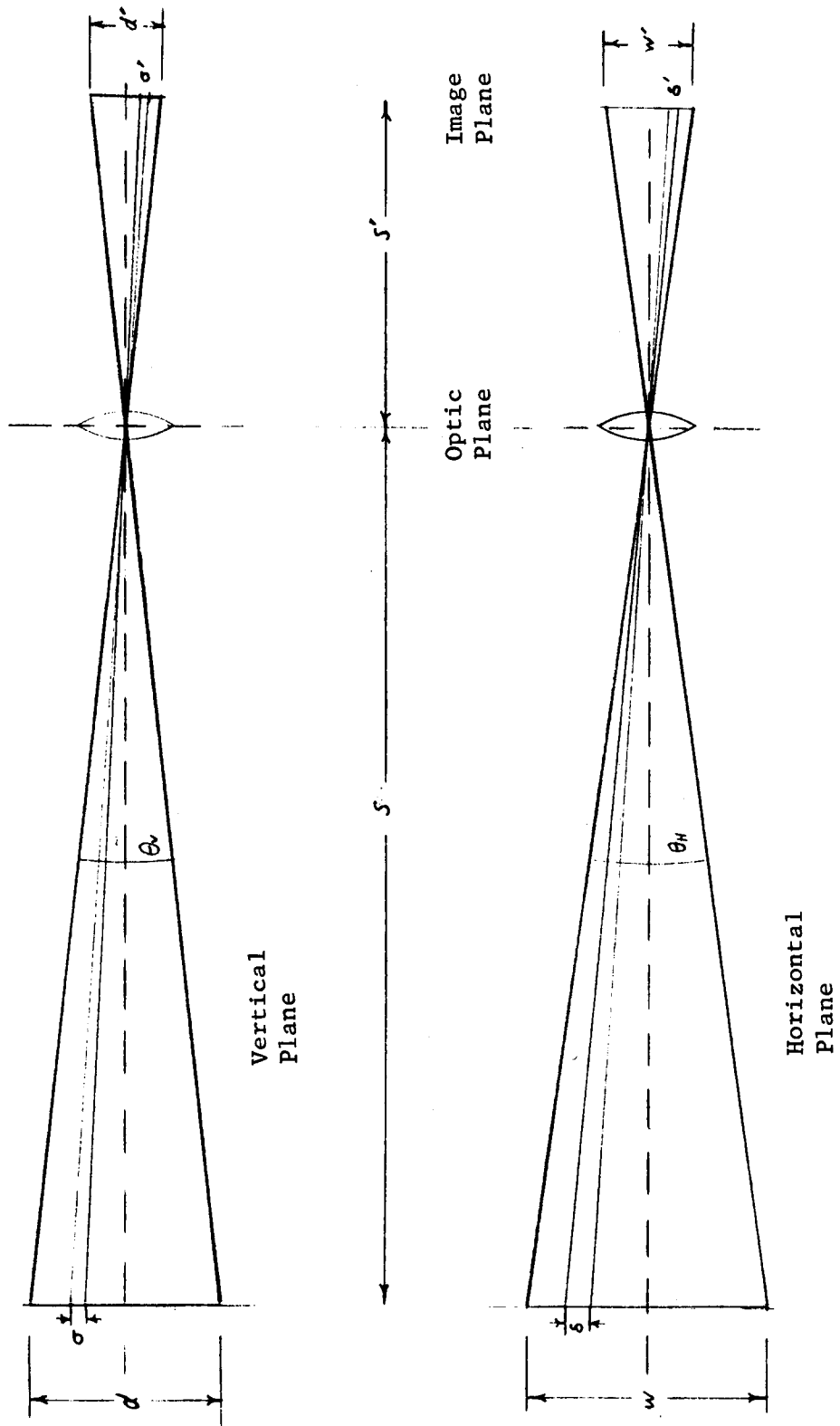


FIGURE 2-2

OPTICAL PARAMETERS



In general,  $d'$  can be found from:

$$d' = \left[ \frac{Ud^2}{A^2+1} \right]^{\frac{1}{2}} \quad (2-6)$$

At a distance  $s$ , the minimum resolvable element  $\sigma$  is to be imaged on the photocathode. In order to determine the lens requirements, the height of  $\sigma'$  must be found, and must equal one line of resolution. The number of lines of resolution must necessarily be less than the number of active scanning lines due to the statistical interference. Several groups have examined this effect with results ranging from 0.53 to 0.85, with the most common value being the Kell factor  $2^{-\frac{1}{2}}$ . A line of resolution must then be  $\sqrt{2}$  times larger than the width of a scanning line, or the number of resolution lines  $N_R$  equals 0.707 the number of active scanning lines.

The height of  $\sigma'$  can now be found as:

$$\sigma' = \frac{d'}{N_R} = \frac{\sqrt{2} d'}{N_a} = \frac{\sqrt{2} d'}{K_v N_t} \quad (2-7)$$

where

$N_R$  = number of lines of resolution

$N_a$  = number of active scanning lines

$N_t$  = total number of scanning lines

$K_v$  = vertical utilization factor

With the object and image sizes determined, the image distance can now be found from

$$s' = s \frac{\sigma'}{\sigma} \quad (2-8)$$

and the required focal length to produce this size image from

$$f = \frac{s s'}{s+s'} \quad (2-9)$$

or directly by substituting for  $s'$

$$f = \frac{s}{1 + \frac{\sigma}{\sigma'}} \quad (2-10)$$

This equation is graphed in Figure 2-3, using a 1" vidicon, 500 lines of resolution, and a square raster ( $A = 1$ ). To resolve the 25 cm crevice example at a distance of 100 meters, a focal length of 444 mm would be required.

In Figures 2-4 and 2-5, the parameter  $\sigma'$  is changed by using a 2" vidicon or a greater number of scanning lines. A 4:3 aspect ratio would necessitate a great focal length. To show the trade off between lines of resolution and optical focal length, the equation is graphed in Figure 2-6, keeping the distance,  $s$ , fixed at 100 meters and using  $\sigma$  as the parameter. The equation used is defined in terms of  $d'$  and  $N_R$ .

Other values of interest can now be found, such as the vertical viewing angle

$\Theta_v$ .

$$\Theta_v = 2 \arctan \frac{N_R \sigma}{2s} \quad (2-11)$$

The value of  $\Theta_v$  can also be found as the product of the angle subtended by the minimum resolvable height (determined in Section 2.1),  $\gamma$ , and the numbers of lines of resolution.

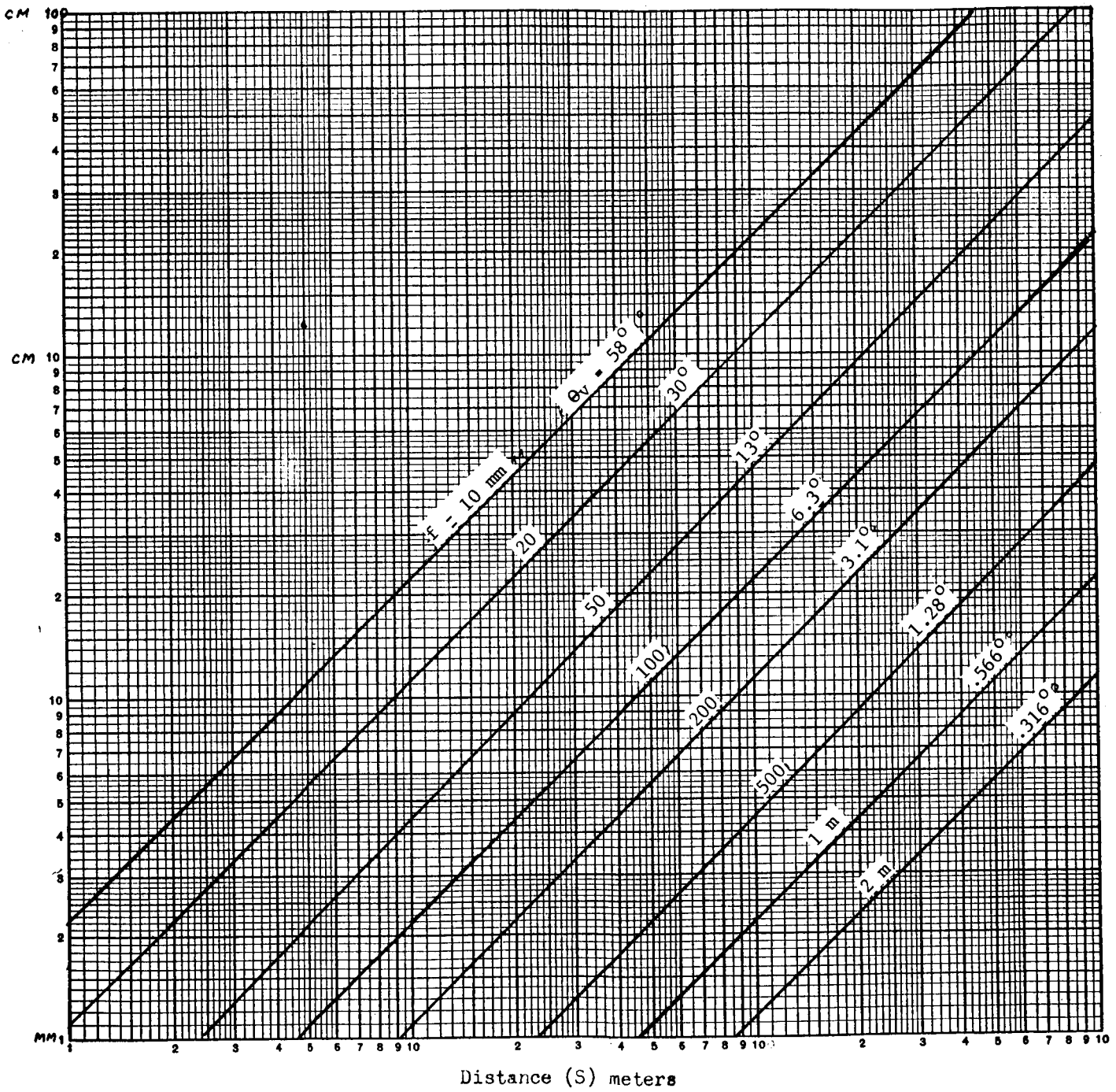


FIGURE 2-3 1" VID 500 = N<sub>R</sub>

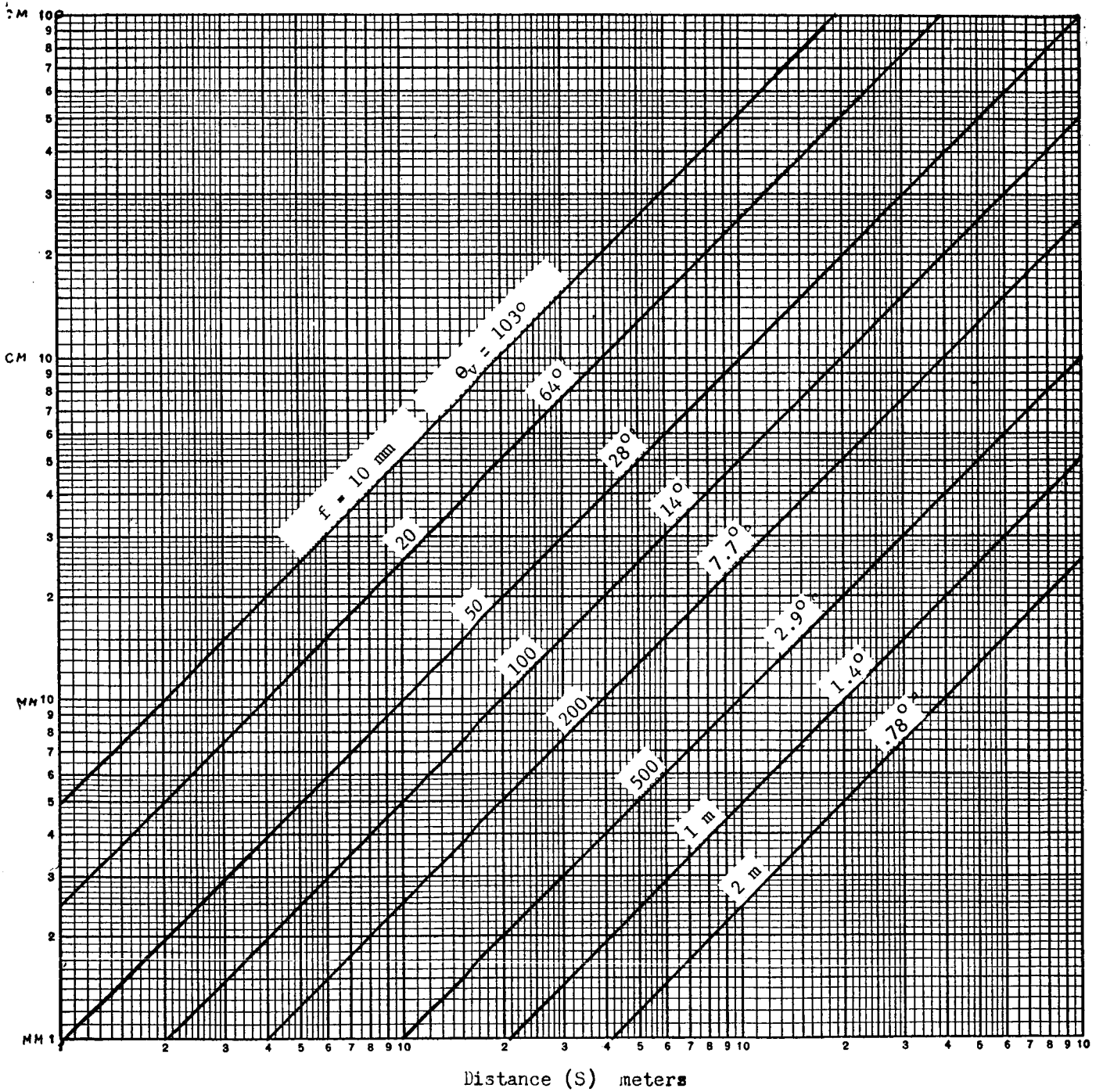


FIGURE 2-4 2" VID 500 =  $N_R$

1" Vidicon Aspect 1:1

650 Lines Resolution

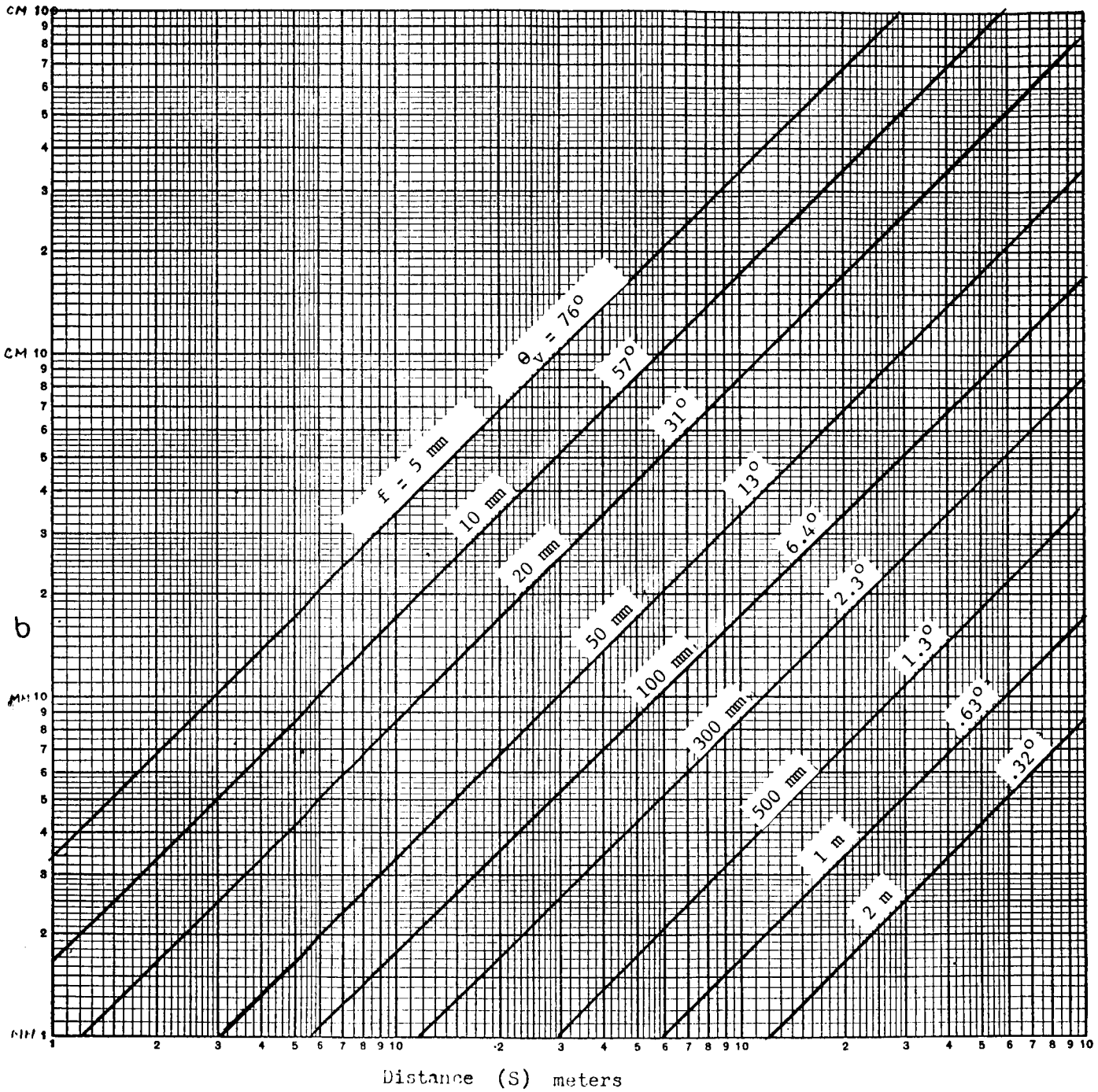


FIGURE 2-5 1" VID 650 =  $N_R$

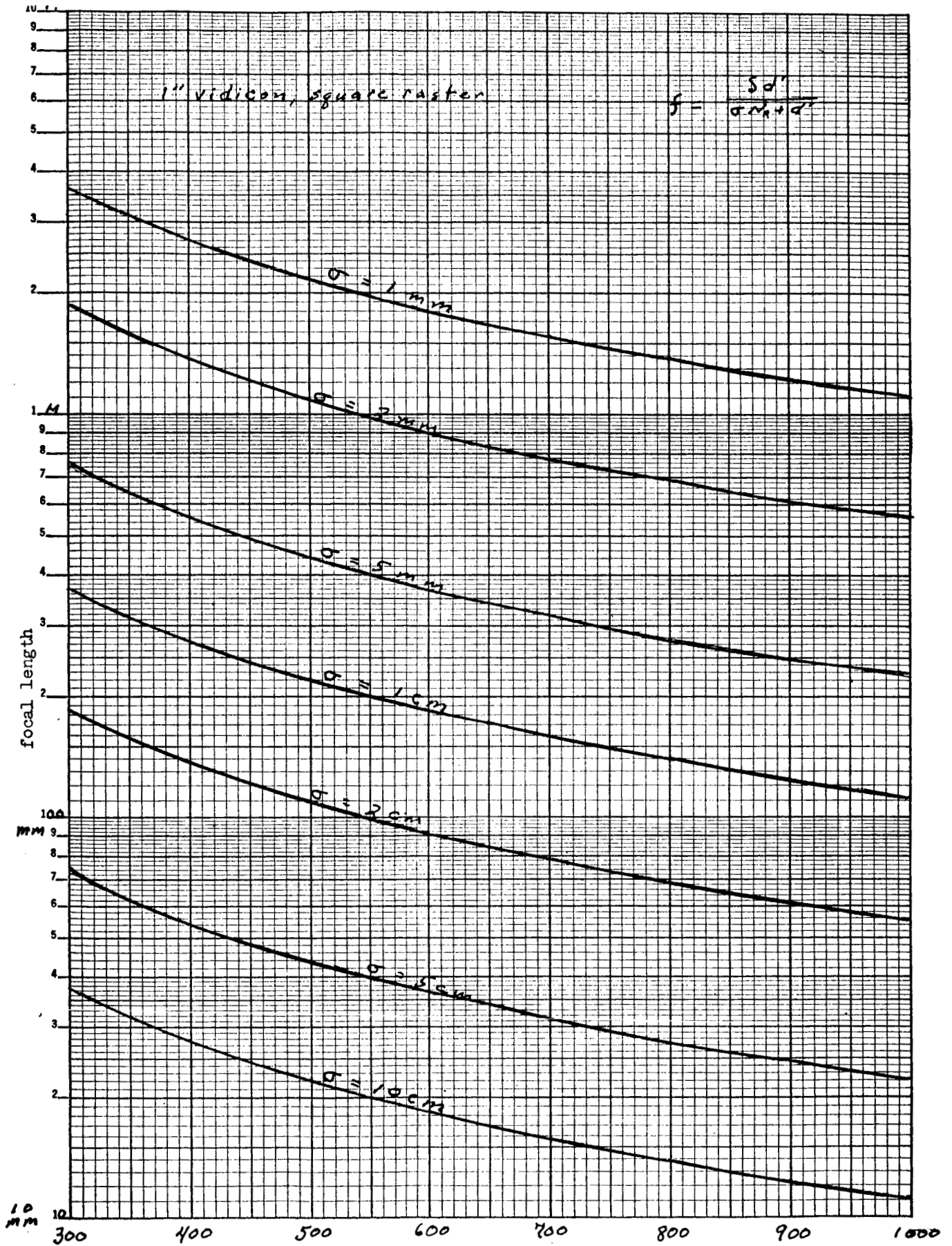


FIGURE 2-6 FOCAL LENGTH VERSUS LINES OF RESOLUTION

The vertical field of view  $d$  can be found from:

$$d = \phi \cdot N_R \quad (2-12)$$

For example, the 25 cm crevice presents a 5 mm height and  $d$  would be only 2.5 meters when using 500 lines of resolution.

The above data has all been done in the vertical plane and assumes that the scanning lines are horizontal. To determine parameters in the horizontal plane, the vertical parameters should be multiplied by the aspect ratio, i.e.,

$$\Theta_H = A \cdot \Theta_V \quad (2-13)$$

$$w = A \cdot d \quad (2-14)$$

The minimum resolvable element in the horizontal plane is an exception in that the resolution ratio  $M$  must be considered.

$$\delta = \frac{\phi}{M} \quad (2-15)$$

where

$$M = \frac{\text{resolution in horizontal plane}}{\text{resolution in vertical plane}}$$

$$\delta = \text{minimum resolvable element in horizontal plane}$$

### 2.3 LENS PHOTOMETRY

To relate the lunar surface brightness as determined in Section 1.5 to the image plane illumination, an expression for the optical system is required. Figure 2-7 shows an object having an area  $A$ , seen by a lens having an area  $A_o$  and producing an image  $A_i$ .

If the object has a brightness  $B$ , then its intensity is  $I = BA$ , which is given as flux per solid angle, lumens/steradian.

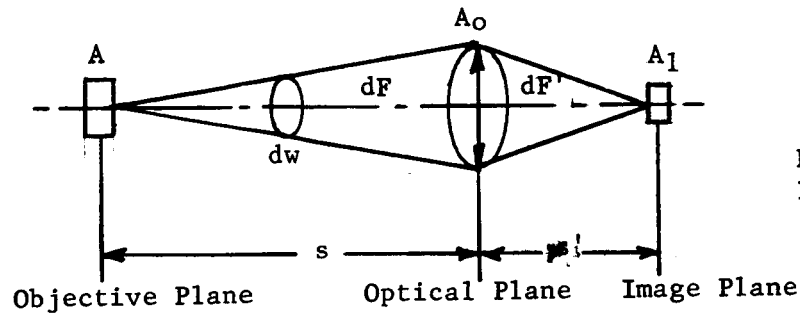


FIGURE 2-7  
LENS PHOTOMETRY

The amount of flux entering the lens surface as  $dF$  is determined by

$$dF = BA \, d\omega \quad (2-16)$$

where  $d\omega$  is the solid angle subtended by the lens surface at the distance  $s$ .

Since the area of the lens is  $A_0 = \pi r^2$  or  $\frac{\pi d^2}{4}$ , the flux entering the lens is:

$$dF = \frac{BA \pi d^2}{4s^2} \quad (2-17)$$

This flux is transmitted through the lens with an optical efficiency or transmittance  $T$ .

The flux that leaves the lens is

$$dF = dF \times T = \frac{BA \pi d^2 T}{4s^2} \quad (2-18)$$

This flux will strike the image plane (photocathode) and produce the image

$A_i$ . By definition, the illumination  $E$  is the flux per unit area.

$$E = \frac{dF'}{A_i} = \frac{\pi B d^2 T A}{4A_i s^2} \quad (2-19)$$



The ratio of an object area to an image area,  $\frac{A}{A_i}$ , is the same as the object distance to the image distance; the quantity squared.

$$\frac{A}{A_i} = \left(\frac{S}{S'}\right)^2 \quad (2-20)$$

Substituting in the equation, it becomes

$$E = \frac{\pi B d^2 T S^2}{4(S')^2 S^2} \quad (2-21)$$

To put the equation in terms of f/no. = F, where  $F = \frac{f}{d}$ ,

$$E = \frac{\pi B f^2 T}{4(S')^2 F^2} \quad (2-22)$$

If the object distance is much greater than the focal length f ( $S > 10f$ ), the image distance approaches the focal length and the equation simplifies to:

$$E = \frac{\pi B T}{4F^2} \quad (2-23)$$

For objects that are off the optical axis, the illumination decreases approximately as the fourth power of the cosine of  $\theta$ , where  $\theta$  is the angle subtended at the lens by the object and the optical axis<sup>2</sup> so that the final equation is:

$$E = \frac{\pi B f^2 T}{4F^2 (S')^2} \cos^4 \theta \quad (2-24)$$

The units for E will depend on the system used for B. If B is in candles per square meter, E will be in lumens/square meter (lux).

Notice that the simplified equation is approximately correct for far objects and optimistic for near objects since the ratio of  $f/s$  is less than one for a positive (converging) lens.

It may be of more interest to put the equation in terms of the object distance instead of the image distance. The illumination then becomes:

$$E = \frac{\pi BT(S-f)^2}{4F^2S^2} \cos^4 \Theta \quad (2-25)$$

Figure 2-8 shows the transfer curves relating the available illumination on the photocathode to the lunar surface brightness. The curves assume a 70% lens transmission which accounts for both absorption and reflection losses at the lens surface. The curves are shown on a "shifted" 5 cycle logarithmic paper in order to include the range of surface brightnesses that will occur under varying conditions. The f/number (F) is used as the parameter and illustrates the large range of aperture control that will be necessary.

The right side of Figure 2-8 shows the brightness variation under several conditions. All curves are based on a lunar albedo of 7%.

Image Plane Illumination vs Scene Brightness  
 for various f/-numbers  
 (Assuming 70% Lens Transmission)

$$E = \frac{\pi B T}{4f^2} = 0.55 B/f^2$$

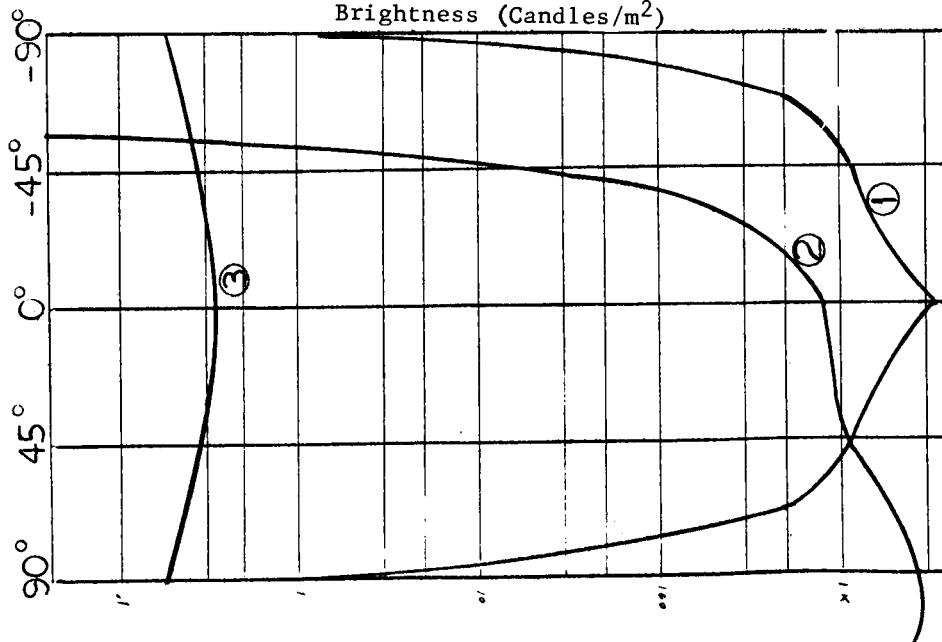
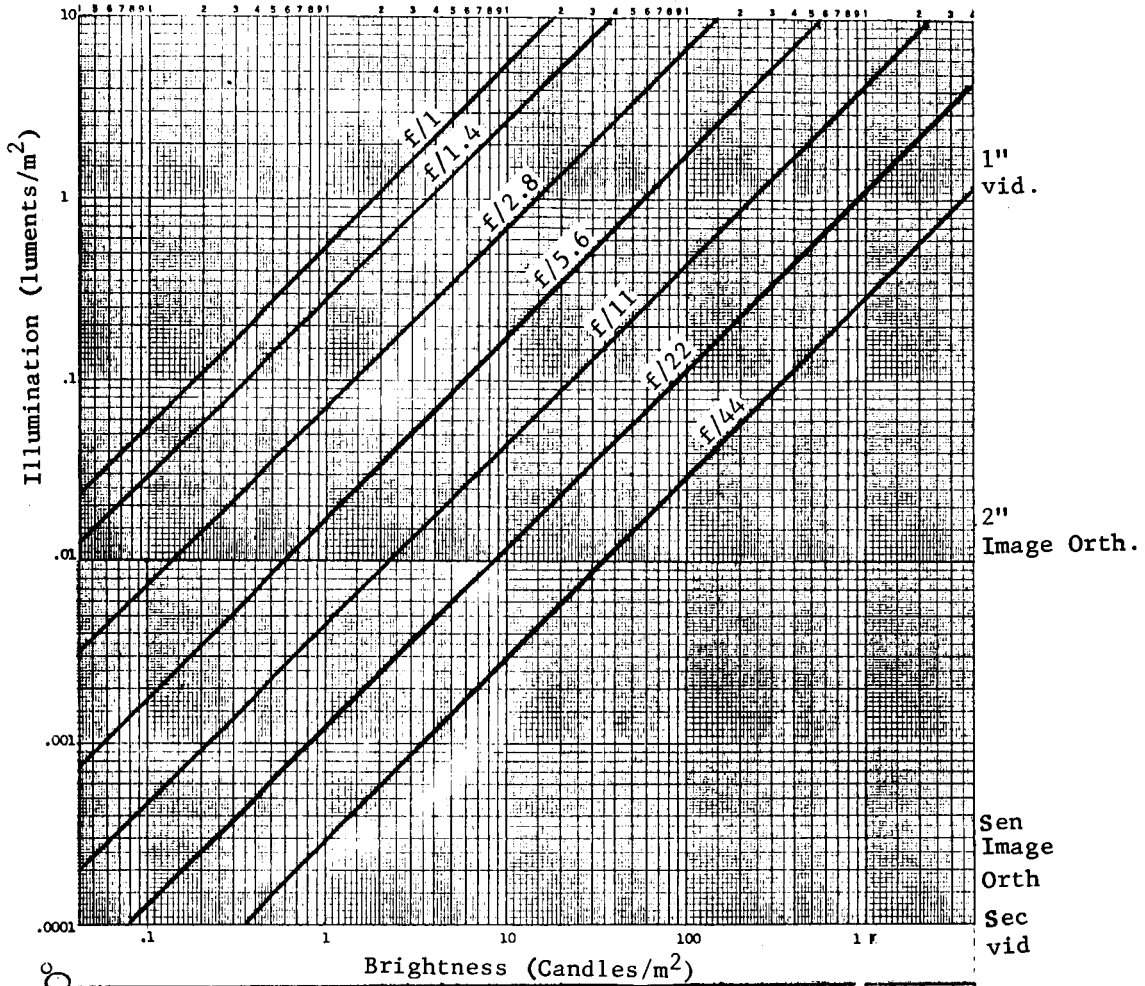


FIGURE 2-8 PHOTOCATHODE ILLUMINATION VS BRIGHTNESS

Curve 1 - Brightness due to direct sunlight at 0° longitude and latitude.

The viewing angle is zero (viewed from the normal)

Curve 2 - The MOLAB headed east at Copernicus - Kepler (Example 1 from Section 1.5)

Curve 3 - The variation in brightness due to earthshine for normal viewing at 0° longitude and latitude.

In starting a pick-up tube sensitivity, several factors must be expressed.

The photocathode illuminations are based on the human eye and would be valid only for a tube that had the same spectral response as the eye. The sensitivity for moving objects is one or two orders of magnitude less than sensitivity when televising a still scene. Due to the integrating capability of the target in some tubes, the exposure time, which would be the time between scans, must also be considered. Finally, the signal/noise ratio must be given.

Along the illumination ordinates, several camera sensitivities have been given in terms of moving objects and frame rates of 10 cps.

## 2.4 APERTURE AND SHUTTER CONTROL

It is expected that the optical system of the television cameras will have a servoed variable aperture system (iris) to compensate for the highly varying brightness levels that will be encountered. This varying brightness will not only be a function of the lunar phase but also a function of the MOLAB heading and the viewing angle of the cameras.

The servo system for the iris would include a photo cell having the same spectral response as the camera sensor and having the same field of view (this could be built in with the camera's optical system). A servo amplifier and the motor-driven iris would complete the servo. A shutter also could be included as a driven element to shut off the optical system if the cameras were aimed directly at the sun (a possibility at certain phase angles and MOLAB headings).

Alternately, the photocathode of the sensor can be used as the photo-cell, and the average current of its video output can be used as the input to the iris servo. A pick-up can be used to control its own sensitivity by varying the voltage applied to the elements. A range of 1000:1 has been achieved with this method. This would not be sufficient for the range of brightnesses expected, so a combination of both methods may be required--both automatic light control and a servoed iris.

### 3.0 BANDWIDTH CONSIDERATIONS

#### 3.1 BANDWIDTH EQUATIONS

The maximum video frequency generated by a scanning system is related to the scanning parameters in the following equation:

$$f = 1/2 \cdot 1/K_H \cdot K_V \cdot A \cdot K_U \cdot M \cdot N_{t1}^2 \cdot f_v \quad (3-1)$$

where

$$K_H = \text{Horizontal utilization factor } \frac{t_f}{t_h}$$

$$K_V = \text{Vertical utilization factor } \frac{N_a}{N_{t1}}$$

$$A = \text{Aspect ratio } \frac{\text{width of raster}}{\text{height}}$$

$$K_U = \text{Kell factor (.7)}$$

$$M = \text{Resolution ratio } \frac{\text{Horizontal}}{\text{Vertical}}$$

$$N_{t1} = \text{Total number of scanning lines}$$

$$f_v = \text{Vertical frame rate (cps)}$$

The maximum video frequency  $f$  will be generated by the scanning of a horizontal element  $\xi$  that is just resolvable.

If the equation is desired in terms of lines of resolution, and

$$N_R = N_{t1} \cdot K_V \cdot K_U \quad (3-2)$$

then

$$f = \frac{A f_v M N_R^2}{2 \cdot K_V \cdot K_U K_H} \quad (3-3)$$

where

$$N_R = \text{Number of lines of resolution}$$

Also, in terms of active lines,  $N_a$ ,

$$f = \frac{AK_u N_a^2 M f_v}{2 K_H K_V} \quad (3-4)$$

The horizontal utilization factor  $K_H$  is defined in Figure 3-1. By maximizing  $K_H$ , the bandwidth can be reduced slightly. This will mean keeping the horizontal retrace time small. The NTSC standard (commercial) states that horizontal blanking is 0.18 H maximum; therefore, 18% of one scanning line, making  $K_H = 0.82$  and  $1/K_H = 1.22$ . To decrease this factor and lower the bandwidth would only mean a sacrifice of increased power in the horizontal sweep circuits.

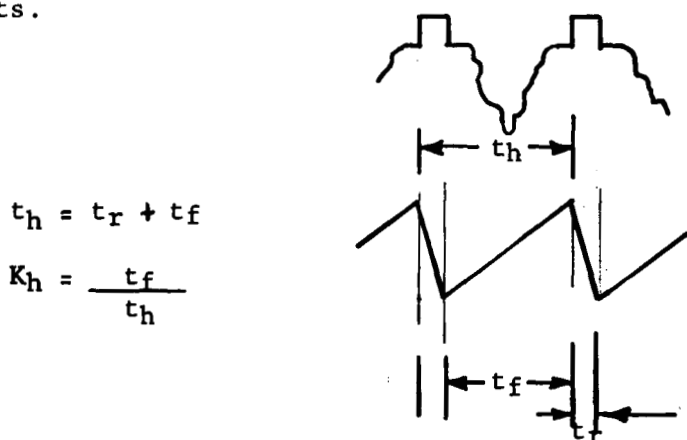


FIGURE 3-1  
VIDEO SIGNAL

In commercial television, an aspect ratio of 4/3 is chosen to conform with the human eye whose high resolution retinal area (fovea) subtends angles of 40° in the horizontal plane and 30° in the vertical plane. In this application, therefore, as the sensing element in the control loop for navigation, it is conceivable that a greater vertical field of view would be required to "see" ahead rather than to the side. An aspect ratio of 1:1 might be used.

### 3.2 FRAME RATE VS VEHICLE VELOCITY

If a low frame rate is used for the television link, the adverse effects on the servo control loop must be considered. Figure 3-2 shows the time sequence from the time when an obstacle is first resolvable to the time when a corrective control signal can first be applied.

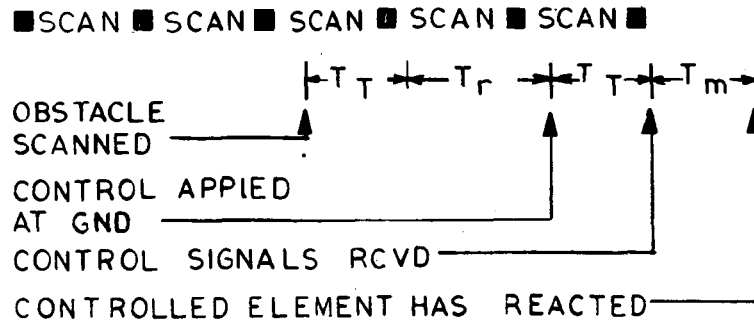


FIGURE 3-2 DELAY TIMES IN CONTROL LOOP

The total time consists of the sum of two earth-moon transit times, the operator reaction time, the mechanical reaction time, plus twice the time for a television frame. With a frame rate of 10 cps, the total delay time is increased by 0.2 seconds; a 4.3% increase. This delay time must be minimized for good control operation, but if the frame rate exceeds 10 frames per second, it is no longer a factor. A minimum  $f_v$  of 10 cps is then established with a maximum  $f_v$  to be determined by the allowable maximum bandwidth that can be transmitted.

A critical distance ( $d_c$ ) can also be determined from Figure 3-2. (The critical distance is defined as the minimum distance at which an obstacle must be resolved in order to avoid said obstacle.) This distance will be the distance travelled during the delay time of the control loop plus the minimum turn radius,  $r_m$ . For the MOLAB VII vehicle,

$$r_m = 7.05 \text{ meters}$$

The maximum speed is expected to be 4.5 meters/second (10 mph) while manned, but in the unmanned mode (when television is used for control) the speed is expected to be 1.5 meters/second (3.3 mph).



Using these values, then, the critical distance when turning to avoid an obstacle is:

$$d_c = v \left[ 2t_t + t_R + t_m + \frac{2}{f_v} \right] + r_m \quad (3-7)$$

$$d_c = 1.5 \left[ 4.84 \right] + 7.05 = 14.26 \text{ meters}$$

$$t_t = \text{earth moon transit time} = 1.32 \text{ second}$$

$$t_R = \text{reaction time (operator)} = 1.0 \text{ second}$$

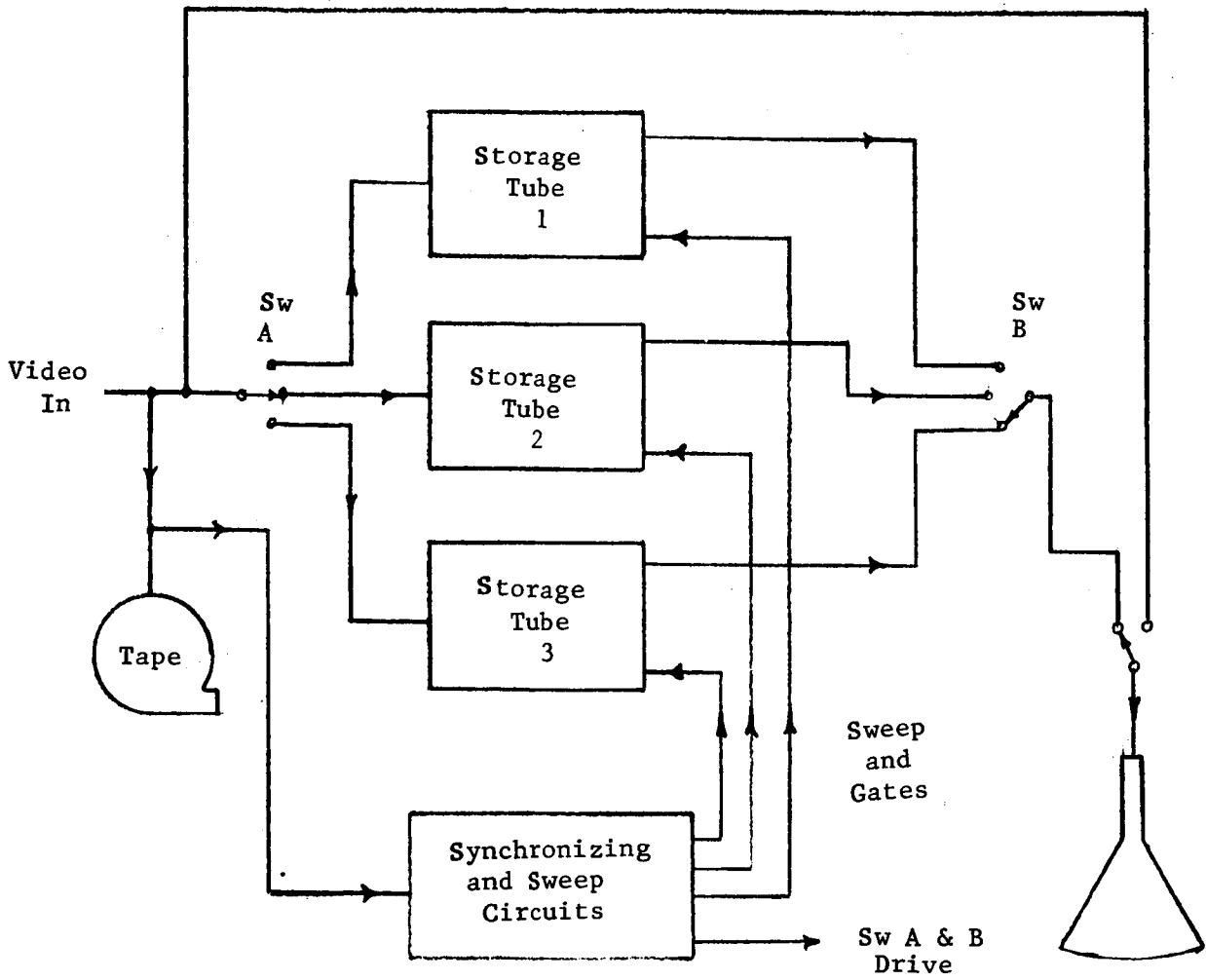
$$t_m = \text{mechanical response time for steering mechanism} - 1.0 \text{ second}$$

$$f_v = \text{vertical frame rate} - 10 \text{ cps}$$

If the  $\frac{2}{f_v}$  term had been ignored, the critical distance would have been 14.01 meters.

The low frame rate of 10 cps is, of course, below the critical flicker frequency for all practical contrast ratios. If it is deemed necessary to eliminate the flicker, a scan converter may be used. Figure 3-3 illustrates such a system described by P. J. Rousculp and W. S. Pope<sup>11</sup>, where the scan conversion takes place in the three storage tubes. The writing takes place at line and field frequencies of the incoming video, while the read beams operate at the higher sweep rates. The two switches operate in synchronism but out-of-phase, according to the chart. If the incoming video was at 10 frames/second, one storage tube would supply the video to the monitor for  $\frac{30}{10}$  or 3 frames.

Notice that this system does not increase the complexity of the MOLAB circuits, but only those of the ground station. The operator should have the ability



Stor. Tube	1	R	E	W	R	E	W	
	2	W	R	E	W	R	E	
	3	E	W	R	E	W	R	
		1	2	3	4	5	6	t → t = $\frac{1}{f_v}$

W = Write - Slow Sweep Writing Beam On  
 R = Read - Fast Sweep Reading Beam On  
 E = Erase Prime Storage Surface

FIGURE 3-3 SCAN CONVERTER BLOCK DIAGRAM

Rousculp & Pope

to choose either the original video or the converted video for his presentation.

### 3.3 RESOLUTION RATIO

Once the scanning parameters such as  $N_{t1}$ , frame rate, aspect ratio, and utilization factors have been set, the maximum video frequency generated is determined by the resolution ratio  $M$ . If the video information is transmitted through a system (such as the RF link) having a lower cut-off than the value of  $f$  using an  $M = 1$ , the horizontal resolution will be proportionally limited.

Regarding obstacles, it appears that the greater resolution would be needed in the vertical direction. A loss in horizontal resolution would mean "blindness" to a narrow vertical object such as a pole, but would not mean the inability to resolve the vertical edge of a cliff. Loss of resolution in the vertical direction would cause blindness to a narrow horizontal line such as the appearance of a crevice. The crevice, of course, is more to be expected than the pole (unless the pole were man-made). For this system then, using horizontal scanning lines, a resolution ratio of 0.5 to 0.75 may be satisfactory.

### 3.4 GRAPHS

Bandwidth versus frame rate equations have been graphed in Figures 3-4 through 3-7 to facilitate bandwidth determination in terms of either total scanning lines or resolution lines. Two aspect ratios have been shown for

Bandwidth vs. Frame Rate vs. Lines of Resolution

$$f = \frac{N_R^2 f_v}{1.105}$$

Aspect Ratio 1/1

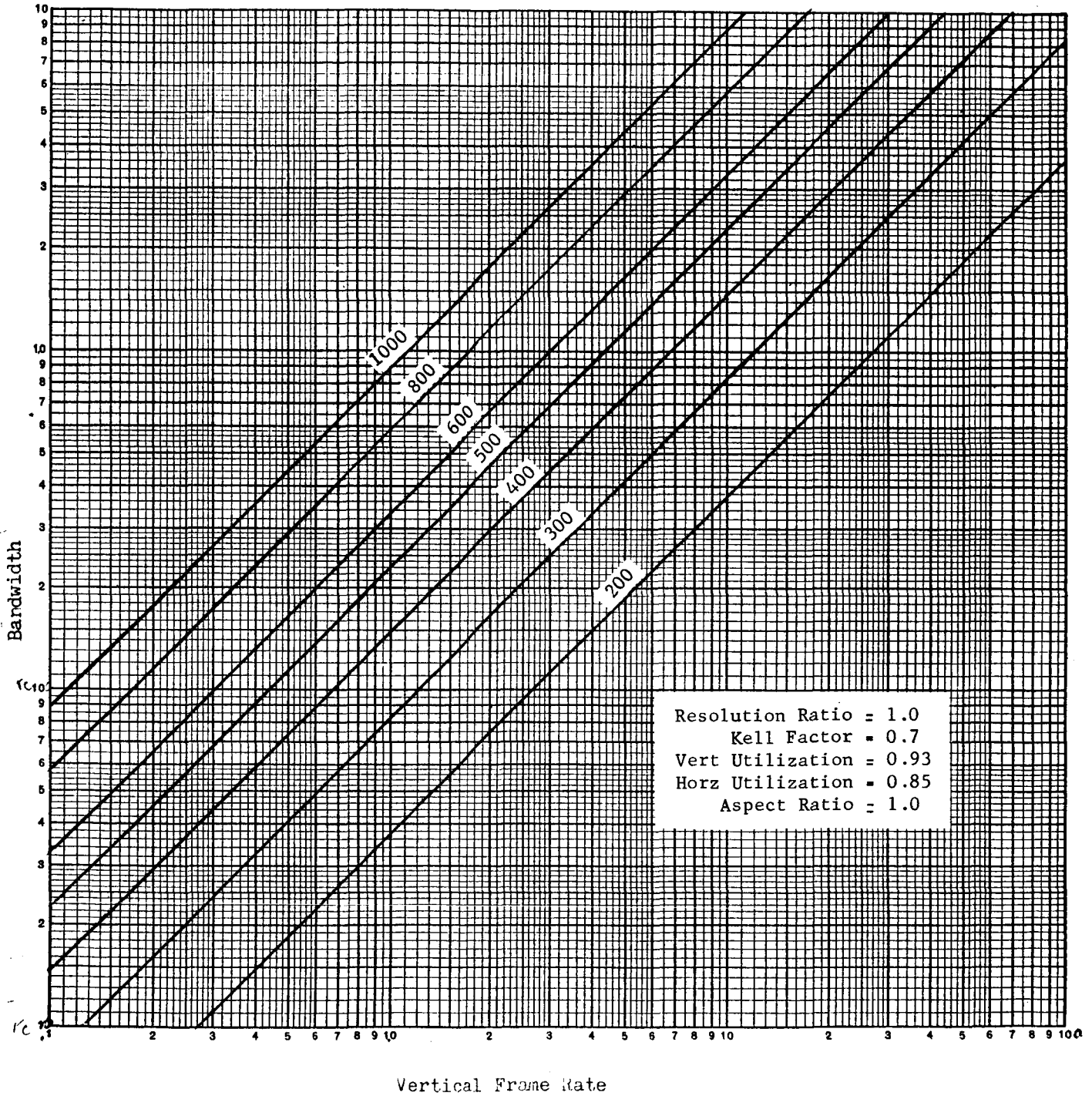


FIGURE 3-4 BANDWIDTH CHART

Bandwidth vs. Frame Rate vs. Lines of Resolution

$$f = .413 N_R^2 f_v$$

Aspect Ratio 1/1  
Resolution Ratio 0.5

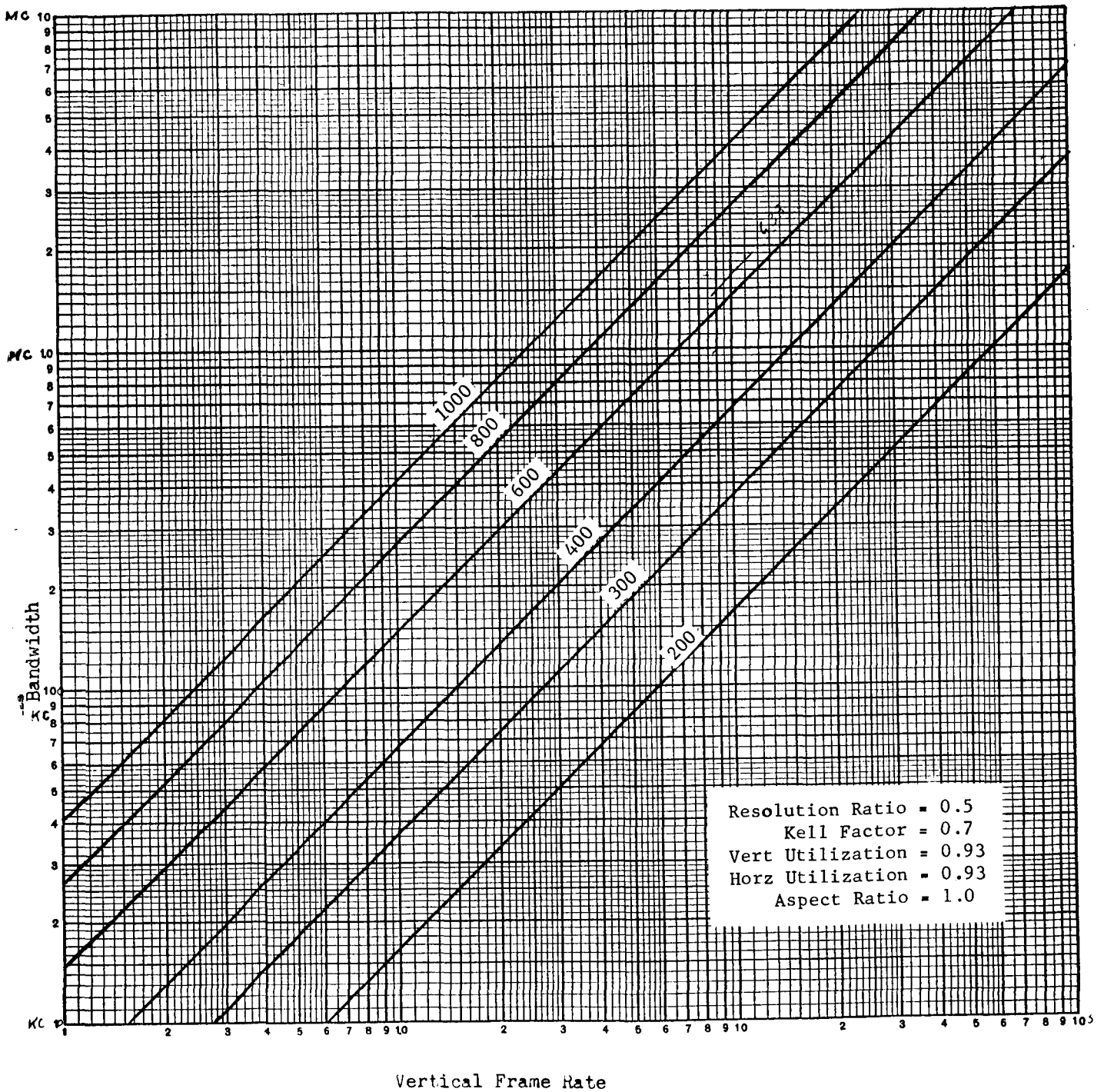
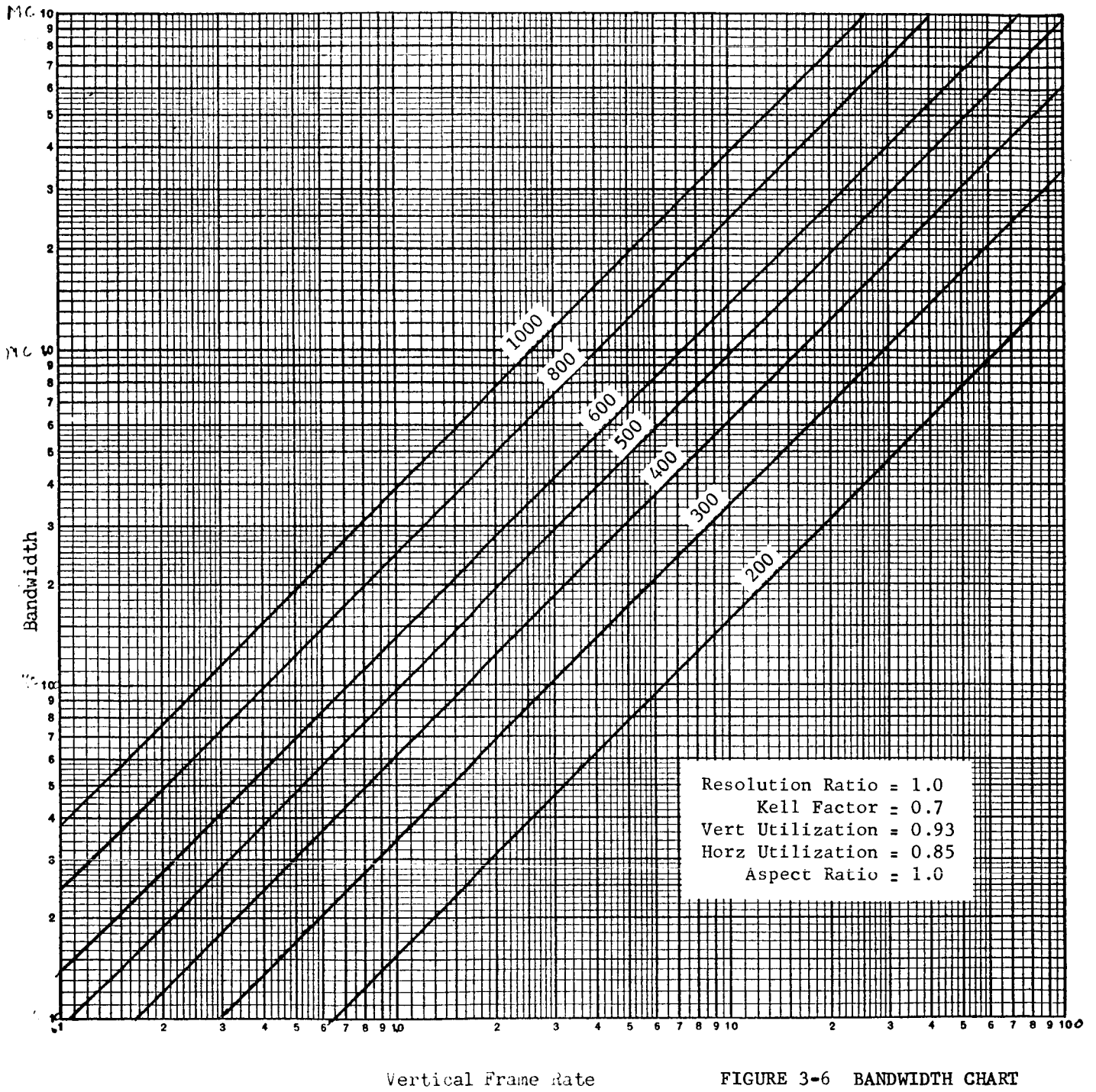


FIGURE 3-5 BANDWIDTH CHART

Bandwidth vs. Frame Rate vs. Total Scanning Lines

$$f = .393 N^2 f_v$$

Aspect Ratio 1/1



Resolution Ratio = 1.0  
 Kell Factor = 0.7  
 Vert Utilization = 0.93  
 Horz Utilization = 0.85  
 Aspect Ratio = 1.0

Vertical Frame Rate

FIGURE 3-6 BANDWIDTH CHART

$$f = \frac{1.33 N_v^2 f_v}{1.105}$$

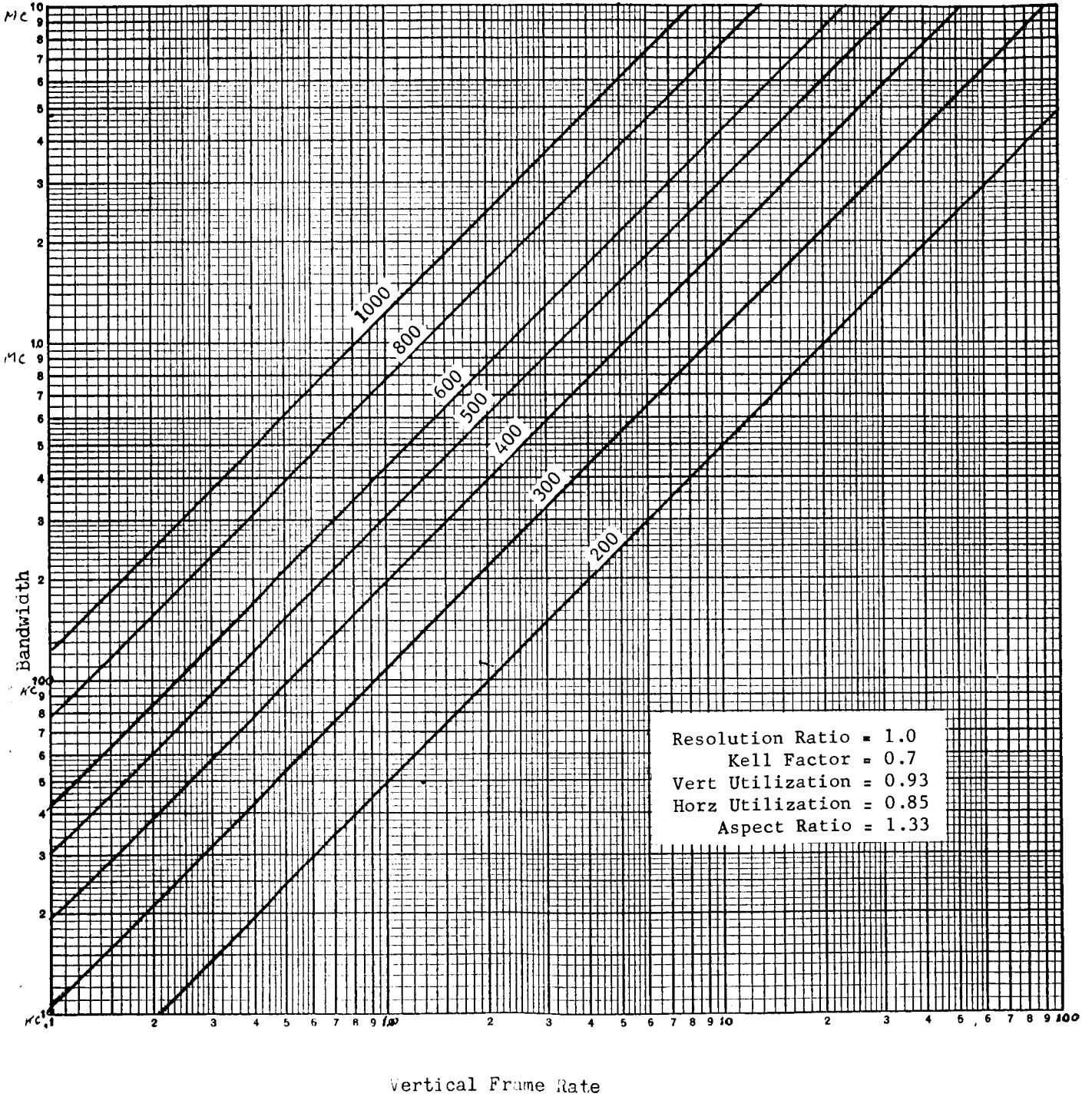


FIGURE 3-7 BANDWIDTH CHART

the resolution line charts. Figure 3-5 represents a minimal bandwidth condition by using a high value of horizontal utilization factor and a low resolution ratio of 0.5.

An example of parameters from this graph could be derived as follows:

- a) Assume an allotted RF bandwidth of 8 mc and a FM modulation system using a modulation index of 2. The maximum video frequency in the modulating signal would be 1.65 mc.
- b) The minimum frame rate was established as 10 cps. From Figure 3-5, the number of lines of resolution would be 633 and from Figure 2-6, the focal length required to see the 25 cm crevice at 100 meters would be 350 mm.
- c) Since this is based on a 0.5 resolution ratio, the minimum horizontal width that could be resolved would be

$$\frac{5\text{mm}}{.5} = 10 \text{ mm}$$

### 3.5 STEREOPTICS

If the television link is considered of such importance that it be made redundant, then it is feasible to consider a stereoptic (three dimensional) video system. The system would consist of two separate cameras and video chains with mixing of signals just prior to modulation. At the ground station, separation of left and right video would be accomplished, and stereo display



would be provided to the operator. He would also have the capability of selecting a combined monoscopic display.

On the failure of any part of either camera chain, the remaining camera could still deliver a monoscopic picture. The entire system would be nonredundant stereo and redundant monoscopic. This assumes that a loss of stereoptics does not prevent the operator from controlling the MOLAB due to the loss of depth perception.

The duality of the human eyes permits ranging and the stereo effect for distances up to a few feet. By increasing the separation between the optical axes of the camera lens objectives, a synthetic stereo effect can be created for greater ranges with an accompanying increase in the distortion of near objects. The optimum spacing can be determined empirically as it is based on the psychovisual effect.

If the video is mixed and presented on a single monitor, the two optical systems must be carefully aligned and a single synchronizing system used for optimum results.

### 3.6 RANGE FINDING

If range finding is to be accomplished with the two-camera system, the following parameters must be considered:

- a) Allowable range error at the maximum range.
- b) The minimum range at which range finding is to be accomplished.
- c) The separation of the lens system's objectives.

$$dr = \sec^2 \left[ \arctan \frac{r}{x} \right] \frac{d\alpha}{57.3} \quad (3-14)$$

The range error  $dr$  is then related to the angular error of the mirror setting  $d\alpha$  for small values of  $d\alpha$ , and for any given value of range and separation.

In order to express the range error in terms of the readout dial error, equation 3-12 is rewritten in terms of  $d\alpha$  and  $d\alpha_R$ , and substituted in equation 3-14. The range error is then:

$$dr = \sec^2 \left[ \arctan \frac{r}{x} \right] \frac{90 - \arctan \frac{r_{\min}}{x}}{20630} d\alpha_R \quad (3-15)$$

where

$r$  is range in meters

$x$  is separation in meters

$r_{\min}$  is minimum range capability

$dr$  is the range error in meters

$d\alpha_R$  is the resolving capability of the readout dial (in degrees)

The above assumes that the full  $360^\circ$  is available in the readout dial. If the dial has a dead space, the 20630 term becomes:

$$57.3 (360 - \alpha_d)$$

where  $\alpha_d$  is the unusable portion of the dial.

Equation 3-15 is graphed in Figure 3-9 and shows the range error to be expected for a given resolution of the readout dial. All curves assume an

From these values, the resolution of the readout system can be derived.

Figure 3-8 shows the basic geometry of the range finder, and the basic range equations:

$$r = x \tan \alpha \quad (3-8)$$

$\alpha$  has maximum value of  $90^\circ$  and a minimum value established by the minimum range  $r_{\min}$ .

$$\alpha_{\min} = \arctan \frac{r_{\min}}{x} \quad (3-9)$$

The range of  $\alpha$  then is  $90 - \arctan \frac{r_{\min}}{x}$  (3-10)

This range will then be coupled through a gear train to drive a  $360^\circ$  dial for readout purposes. The gear train ratio  $N$  will be:

$$N = \frac{360}{\alpha_{\text{range}}} = \frac{360}{90 - \arctan \frac{r_{\min}}{x}} \quad (3-11)$$

and the two angles  $\alpha$ , the mirror angle and  $\alpha_R$ , the readout angle -- are related by

$$\alpha \cdot \frac{360}{90 - \arctan \frac{r_{\min}}{x}} = \alpha_R \quad (3-12)$$

For relating the errors in the system, the differential of the basic range equation is found:

$$dr = x \sec^2 \alpha d\alpha \quad (3-13)$$

where  $d\alpha$  is expressed in radian measure.

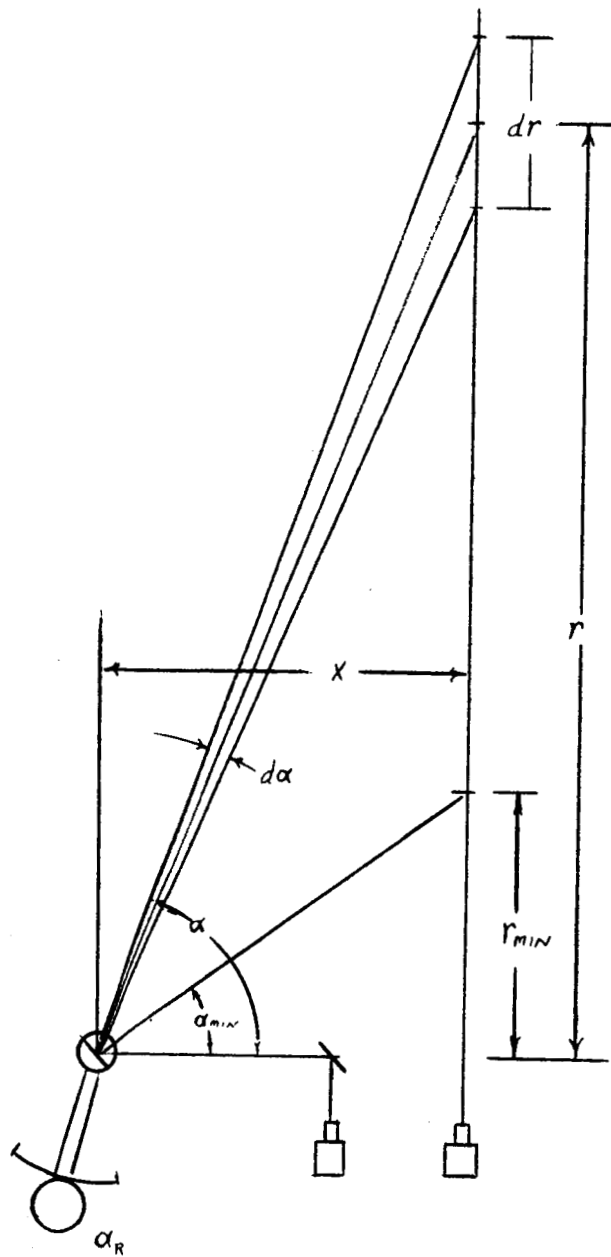


FIGURE 3-8 RANGE FINDER GEOMETRY

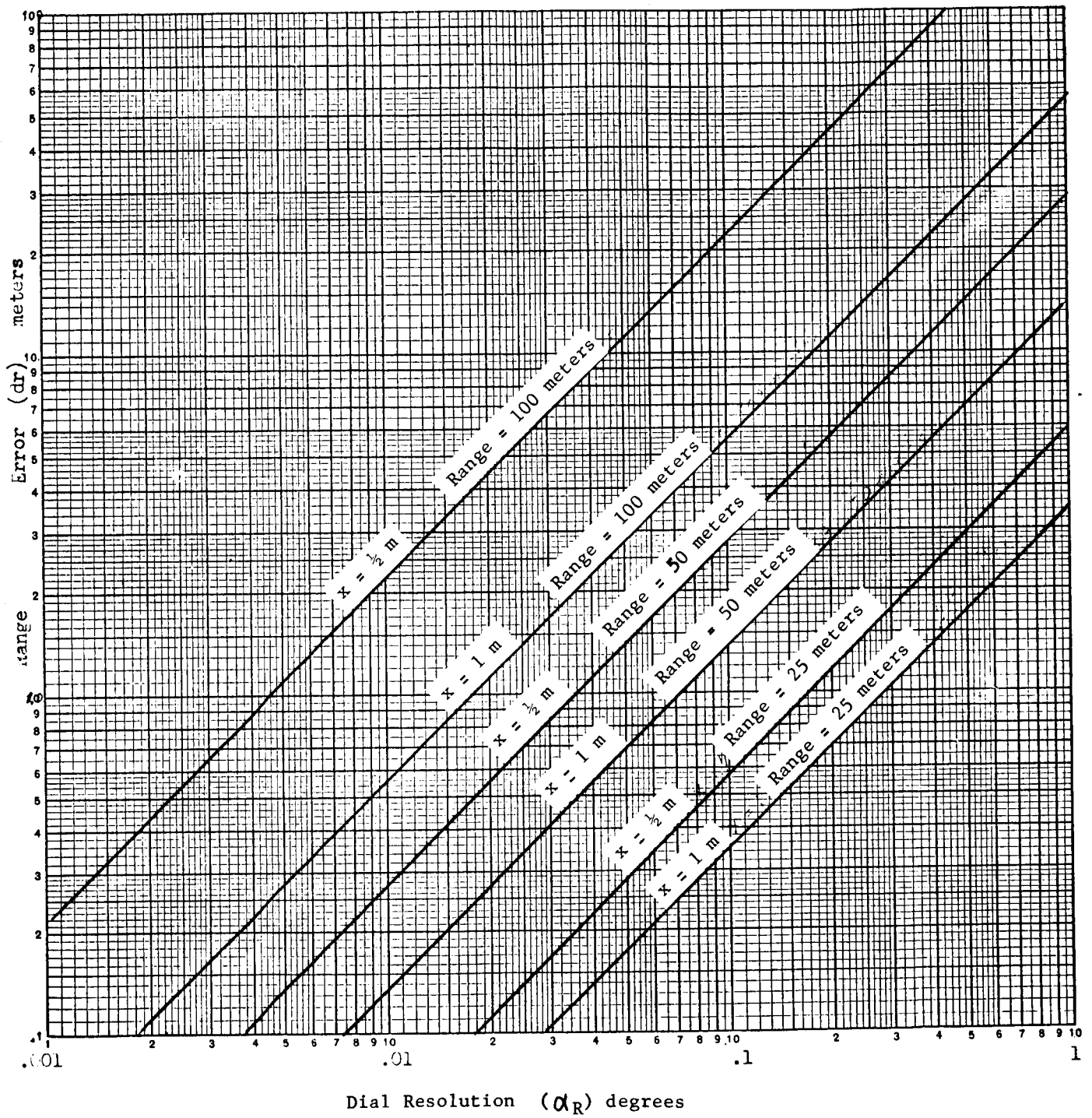


FIGURE 3-9 RANGE FINDER ERROR GRAPH

$r_{\min}$  of 5 meters, and a non-backlash gear train coupling the movable mirror and the readout dial.

It is expected that the apertures of the cameras will be in the horizontal plane in which the ranging of objects can present a near vertical and contrasting image. The range finder would not be useful for a crevice laying normal to the path of the vehicle.

The two opposing constraints of wide separation for range finding and close apertures for stereoptic view at close ranges would dictate a compromise. The problem may be solved empirically by separating the apertures until intolerable distortion occurs.

### 3.7 BANDWIDTH REDUCTION

It is a fundamental principle of information theory that an exchange can be made between time and bandwidth. This principle is used in a bandwidth reduction system where the video is recorded and then read and transmitted at a slower rate. In this application, the increased delay time could not be permitted when the television is performing its prime function of the sensor in the driver's control loop.

A second approach to this problem is based on a more effective use of bandwidth by analyzing the video signal and its frequency spectrum. By processing the video signal, either a greater amount of information can

be transmitted in the same bandwidth or the same amount of information can be transmitted in a reduced bandwidth. In conventional television, the brightness of every element is transmitted. In the processed system, only the brightness changes and the position of these changes are transmitted. This system will cause a reduction in bandwidth only if the number of brightness changes is considerably less than the total. Statistical analysis of even high definition pictures shows that this is true, and systems which produce a reduction of 50% have been created.

In a paper by Newell & Geddes<sup>12</sup>, a series of tests were made on three systems based on this method. The following was extracted from the conclusion of this paper (page 313):

"The quality of reproduction was in each case noticeably inferior to that which can be achieved with the conventional system.... A useful reduction could not be achieved by such techniques without imposing new restrictions on the amount of fine structure in the picture."

The purpose of this system is to present a true picture of the lunar surface and not just a pleasing picture. Therefore, the present equipment for bandwidth reduction is not satisfactory in this application. This is based not only on the degradation of picture quality but also on the increase of equipment complexity. While the principles are sound, the present equipment is lacking and future efforts may produce an acceptable system.

## 4.0 ARTIFICIAL ILLUMINATION

### 4.1 PHOTOCATHODE ILLUMINATION

It has been seen that the natural illumination sources will not be sufficient for adequate video pictures at all phases of the moon. Due to the lack of atmosphere, shadowed areas will appear very dark and will require some artificial illumination. It then becomes necessary to establish the intensity, beam width, spectrum, and position of the lamps.

It was seen in Section 1.0 that the brightness of the lunar surface due to an illumination  $E$  was:

$$B = \frac{E}{\pi} \rho \phi \quad (4-1)$$

If the lights are mounted at the same position as the camera apertures, the value of  $\phi$  will be approximately unity. Even for small difference angles  $\alpha = 5^\circ$ , the photometric function falls off rapidly.

The value of  $E$  will be a function of the lamp parameters, lumped as the effective intensity  $I_E$ , and the distance(s) involved. The brightness is now:

$$B = \frac{I_E \rho \phi}{\pi s^2} \cos \Delta \quad (4-2)$$

where

$$\Delta = \text{angle of the light beam to the normal} = \frac{h}{s}$$



The value of the effective intensity produced by the lamp will be a function of the actual intensity, the reflectors surface reflectivity, the transmission efficiency of the glass, and the beamwidth.

With the filament rated in candles, the total flux emitted is:

$$F = 4\pi I \quad (4-3)$$

If this total flux is collected by the reflector and formed into a conical beam, then the flux density is increased by a factor equal to the ratio of:

$$\frac{\text{solid angle of a sphere}}{\text{solid angle of the beam}}$$

The solid angle of the conical beam can be found from its definition:

$$\omega = \frac{\text{curved surface area of a spherical segment}}{(\text{radius of sphere})^2}$$

$\omega$  is the solid angle subtended by an area on a sphere divided by the radius of the sphere squared. The area of a spherical segment (Figure 4-1) can be found from:

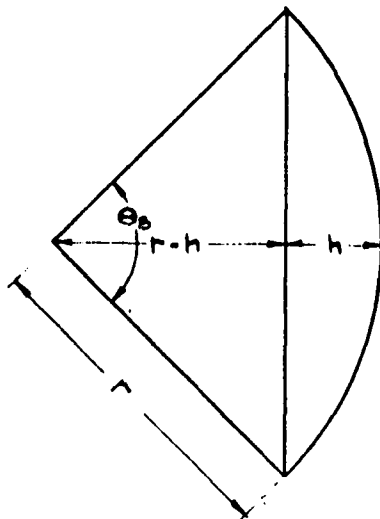


FIGURE 4-1 SOLID ANGLE OF CONICAL SECTION

$$A = 2 \pi r h$$

and

$$\theta_B = 2 \arccos \frac{r - h}{r}$$

Substituting for h

$$B = 2 \arccos \frac{r - \frac{A}{2\pi r}}{r} = 2 \arccos \left( 1 - \frac{A}{2\pi r^2} \right) \quad (4-4)$$

$$\text{and since } \omega = \frac{A}{r^2} \quad (4-5)$$

$$(4-5)$$

$$\theta_B = 2 \arccos \left( 1 - \frac{\omega}{2\pi} \right)$$

or

$$\omega = 2\pi \left( 1 - \cos \frac{\theta_B}{2} \right) \text{steradians}$$

The effective intensity can now be determined as:

$$I_E = \frac{F}{\omega} = \frac{4 I_a}{2\pi \left( 1 - \cos \frac{\theta_B}{2} \right)} = \frac{2 I_a}{1 - \cos \frac{\theta_B}{2}} \quad (4-6)$$

To account for the absorption losses of the reflector and glass, a dimensionless fractional quantity L is used so that

$$I_E = \frac{2 I_a L}{1 - \cos \frac{\theta_B}{2}} \quad (4-7)$$

Using this value of  $I_E$  in equation 4-2, the surface brightness becomes

$$B = \frac{2 I_a L \phi h}{\pi S^3 \left( 1 - \cos \frac{\theta_B}{2} \right)} \quad (4-8)$$

where

- $I_a$  = Actual intensity of lamp (candles)
- $L$  = Reflector losses
- $\rho$  = Lunar albedo
- $\phi$  = Photometric function
- $S$  = Object distance (meters)
- $\theta_B$  = Conical beamwidth of lamp degrees

The electrical power required to produce the light depends on the efficiency of the source given either in watts/candle or lumens/watt. The two ratings are related by:

$$\text{watts/candle} = \frac{4\pi}{\text{lumens/watt}} \quad (4-9)$$

Table 4-I lists several efficiencies of possible sources.

TABLE 4-I EFFICIENCIES OF POSSIBLE SOURCES		
Source	Watts/Candle	Lumens/Watt
Tungsten	1.25	10
Tungsten, Gas Filled	0.5	25
Mercury Vapor Arc	0.3	42
Sodium Vapor Arc	0.28	45

The electrical power (P) required then is:

$$P = I_a E_f \quad (4-10)$$

$E_f =$  efficiency in watts/candle

or

$$P = \frac{4 \pi I_a}{E_f} \quad (4-11)$$

$E_f =$  efficiency in lumens/watt

The efficiencies given are not absolute, but depend somewhat on the temperature of the filament and, therefore, the lamp's power rating. For example, a gas filled tungsten bulb at 50 watts is rated at 10 lumens/watt while a 30kw bulb is rated at 31 lumens/watt. The value of 25 is valid for the wattage ratings expected for this application.

Using the lens photometry equation from Section 2.2, and substituting for B, the complete transfer equation is:

$$E' = \frac{I_a L \phi T h}{2 S^3 F^2 \left(1 - \cos \frac{\theta_B}{2}\right)} \quad (4-12)$$

Assuming that  $L = .5$ ,  $S = .07$ ,  $\phi = 1$ ,  $T = .7$ ,  $F = 1$ ,  $h = 2$  meters

$$E' = .0245 \frac{I_a}{S^3 \left(1 - \cos \frac{\theta_B}{2}\right)} \quad (4-13)$$

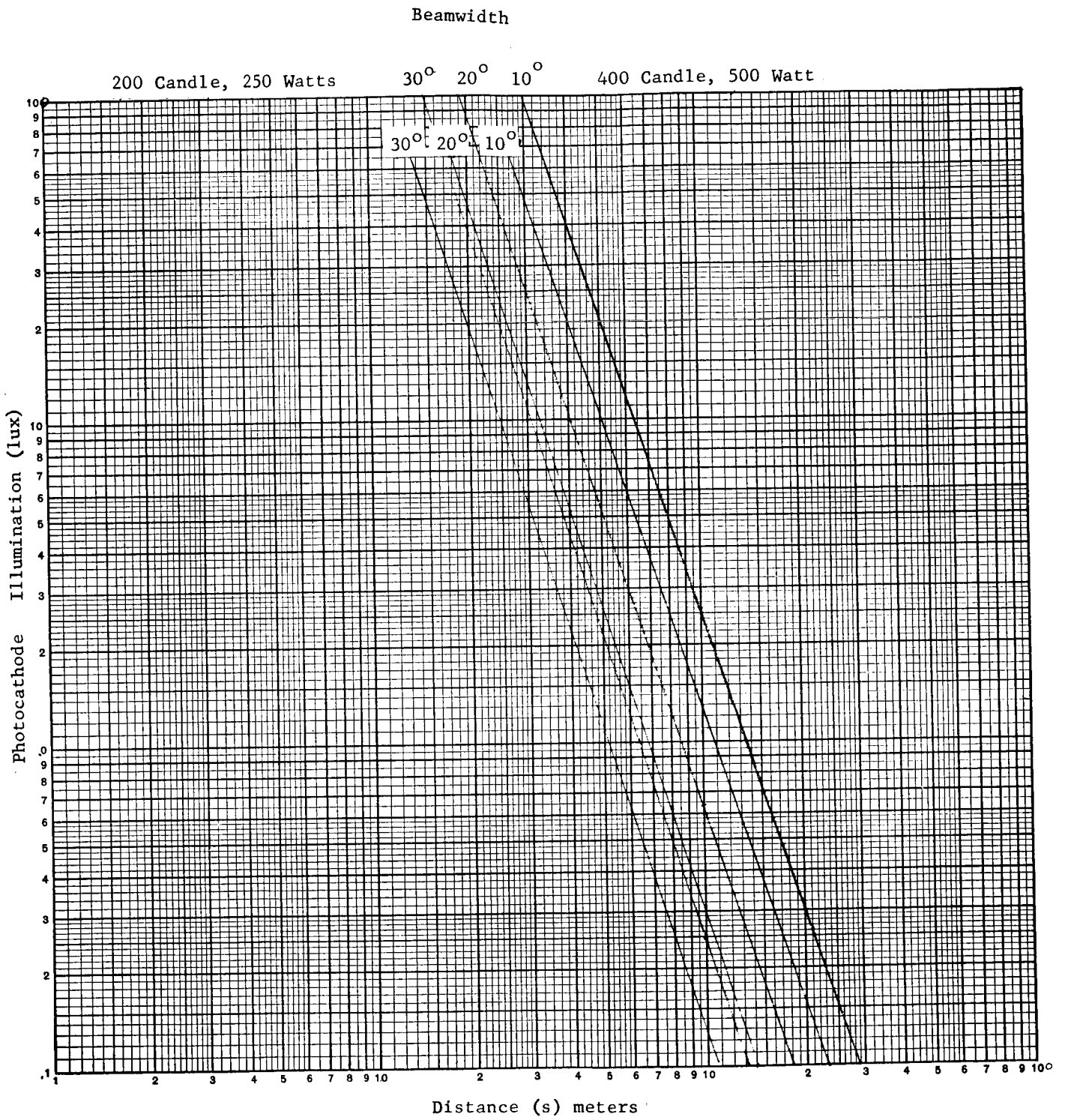


FIGURE 4-2 P.C. ILLUMINATION VERSUS DISTANCE  
ARTIFICIAL ILLUMINATION

Figure 4-2 is a plot of photocathode illumination versus distance for two wattage ratings and three beam widths. The wattage ratings given are those for a tungsten lamp having an efficiency of 10 lumens/watt.

#### 4.2 SPECTRAL RESPONSE CONSIDERATIONS

The efficiencies given in Table 4-I are based on the use of the human eye as the receptor and are only valid for a camera having the same spectral response as the eye. Since this is not probable, the energy must be evaluated in regard to the response curve of the particular device that is used. The procedure is to determine the area under a curve produced by the products of the irradiation and response curves. This is expressed as:

$$G = K \int_0^{\infty} G(\lambda) \gamma(\lambda) d\lambda$$

where

$G$  = Total irradiation in watts/cm<sup>2</sup>

$G(\lambda)$  = Irradiation at a particular wavelength of the source in watts/cm<sup>2</sup>/μ

$\gamma(\lambda)$  = Response of the device at a particular wavelength in amps/watt/cm<sup>2</sup>

$K$  = Constant of proportionality

Since neither the irradiation or response functions can be described

analytically, numerical methods are used in evaluating the integral. To determine the current output of the device, a summation of products is made by:

$$i = \sum_{K=1}^{K=N} G(\lambda)_K \quad \gamma(\lambda)_K$$

A close approximation can be found by using a  $\Delta \lambda = 0.01$  microns. Since  $G(\lambda)$  is given per micron, the answer is  $\frac{1}{\Delta \lambda}$  greater than the computed value. For optimum efficiency, the lamp's energy should be concentrated in the spectral range of the camera tube. In Figure 4-3, the relationship of the solar irradiation, the standard luminosity curve, a typical vidicon response, and a spectrum of a tungsten lamp have been shown. The vidicon is responsive in the shorter and near-ultraviolet region near the peak of the solar irradiation. Much of the energy in the tungsten spectrum is concentrated in the infrared band and would have a low efficiency when evaluated in terms of the vidicon. The outputs of a gaseous conduction lamp, such as mercury vapor and sodium, produce line spectras that are more concentrated in the region of the vidicon and would, therefore, have a higher photocathode efficiency.

In the final analysis, each artificial source (solar irradiation multiplied by the spectral albedo of the moon and the earthshine multiplied by the lunar albedo) must be evaluated by the camera tube's response.

The source of the curves is given as follows:

- 1) Irradiation from the sun, neglecting absorption by atmosphere. Moon, P.<sup>9</sup> p30. Use left ordinates.
- 2) Standard luminosity function. Moon, P.<sup>9</sup> P 52  
Relative, use right ordinates.
- 3) 250 watt tungsten lamp, Moon, P. P 56  
Relative, use right ordinates,  $100 = 10^{-3} \text{ watts/cm}^2/\mu$
- 4) Vidicon Sensitivity. RCA Tube Handbook.  
Relative, use right ordinates,  $100 = .0275 \mu \text{ A}/\mu \text{ W}$



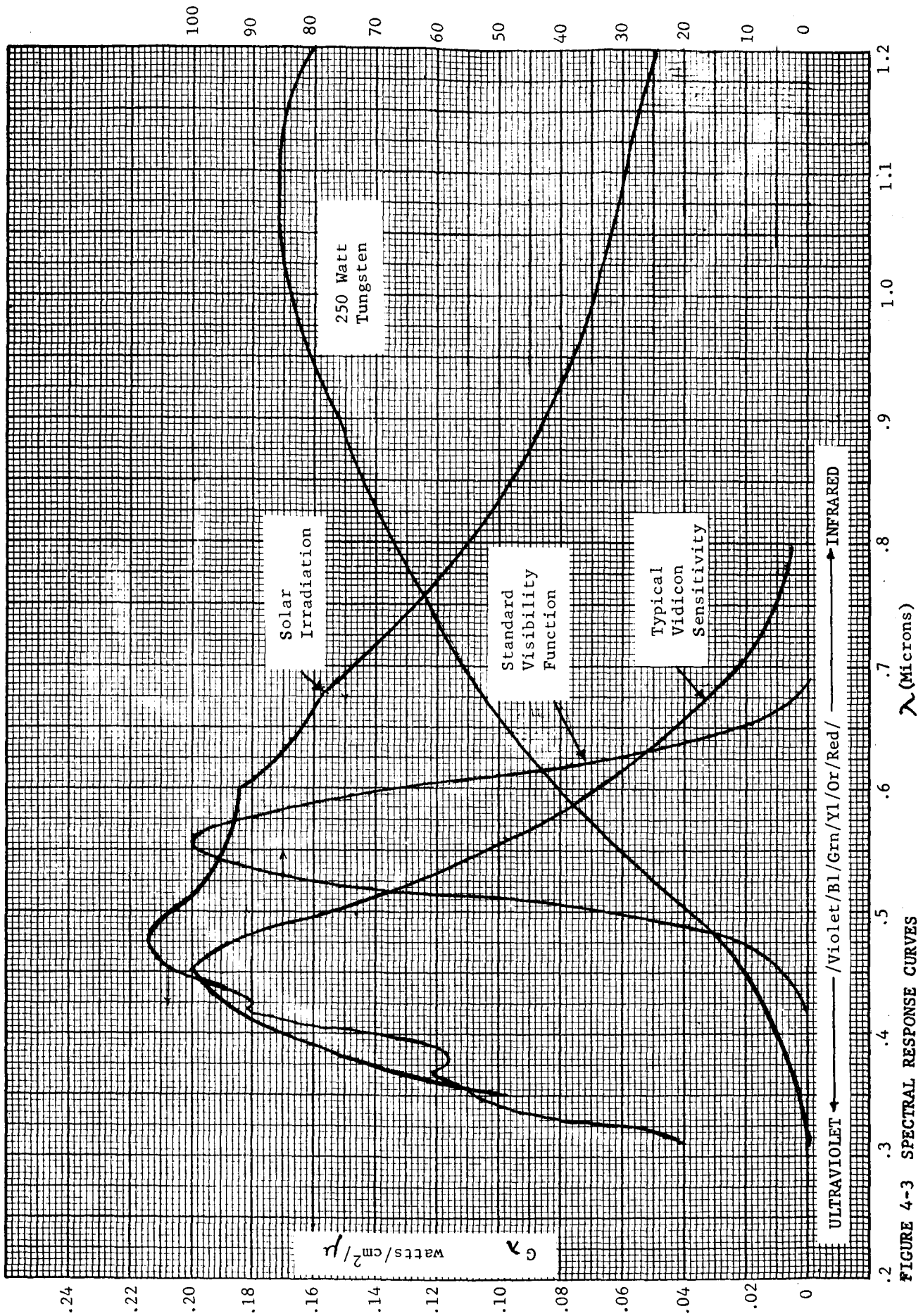


FIGURE 4-3 SPECTRAL RESPONSE CURVES

## 5.0 UP-LINK TELEVISION SUB-SYSTEM

### 5.1 REQUIREMENTS

The purpose of the system must be considered before the parameters of this sub-system can be chosen. The following assumptions are made for the purpose:

- a) This system will be used for transfer of graphic information to the astronauts in order to expedite repair of equipment.
- b) There will be no continuous motion to be considered in the information. However, "step" motion such as would occur in the assembly or dis-assembly of a mechanical device must be considered.
- c) This will not be used on a continuous basis except possibly as a back-up to the main information channels.
- d) The monitor portion of the system may be time-shared with the down link video so that the astronauts can have a local display of the MOLAB's cameras.

### 5.2 SCANNING PARAMETERS AND BANDWIDTH

The scanning parameters will be based on those used in commercial television except for the aspect ratio and frame rate, as follows:

- a) If a square picture (aspect 1:1) is used, then an optimum presentation of page material will be displayed, since it may be aligned either way.
- b) The resolution ratio (M) should be close to unity since equal detail is to be expected in both the horizontal and vertical fields.
- c) A frame rate of approximately 2 cps can be considered sufficient for the display of static material.

Using these values then, the bandwidth can be found from equation 3-1:

with

$$K_H = .9$$

$$K_V = .9$$

$$K_u = .7$$

$$A = 1$$

$$M = 1$$

$$N_T = 525$$

$$f_V = 2$$

then  $f = 193 \text{ KC}$

### 5.3 POWER LEVELS AND RECEIVER QUALITY

Using the MSFN facilities of a 10kw transmitter and an 85 ft parabolic antenna, an estimate of receiver requirements can be made. Of the 10kw

power available, 5kw may be designated for video power, then the receiver power referred to 1 milliwatt,  $P_R$  (dbm), is found from:

$$P_R \text{ (dbm)} = P_T \text{ (dbm)} + G_T + G_R - FS - c - M$$

where

$$P_T = \text{Transmitter power in dbm} = 67 \text{ dbm}$$

$$G_T = \text{Gain of 85' dish (in transmit phase)} = 50\text{db}$$

$$G_R = \text{Gain of 4' receiving antenna} = 25\text{db}$$

$$L_{FS} = \text{Free space loss (at } \lambda = 13\text{cm)} = 212\text{db}$$

$$L_c = \text{Circuit losses (Total)} = 3\text{db}$$

$$M = \text{Design margin} = 3\text{db}$$

Then the signal power at the receiver input is -76dbm.

If a 30db S/N ratio at the output of the demodulator is required for an acceptable picture, a 19db S/N will be required at the receiver input, based on a frequency modulation system with a modulation index of 2.

Using this value to determine the maximum allowable noise at the input  $N_R$ ,

$$N_R = P_R - S/N$$

$$= -76\text{dbm} - 19\text{db} = -95\text{dbm}$$

To determine a noise figure NF from the available signal level and required noise level,

$$NF = N_R - N_d - BW$$

If the noise density is found from

$$N_d = KT$$

using the 290°K temperature of the earth, then  $N_d = -204$  dbw.

The bandwidth, using the value of 200kc from Section 5.2, is 53 db.

The noise figure is then,

$$NF = -95 - (-204) - 53$$

$$NF = -56$$

This shows that requirements of the receiver are not stringent.

#### 5.4 MONITOR

The monitor size is not deemed critical and should conform to available space and weight allotments.

The mointor should have the capability of presenting either the up-link

video (primary) or the output of the local cameras (secondary). The television links are not expected to use exactly the same scanning parameters so some switching may have to occur in the horizontal and vertical sweep circuitry as well as in the video. To prevent unnecessary complications, the up-link system aspect ratio should conform to the primary system (down-link video).

If the monitor is operated at two different frame rates, 10 cps and 2 cps, the phosphor should be acceptable for both. This may require a two layer type such as P-7, with the beam current switched to a lower value when the higher frame rate is being used. Rather than making a compromise, the primary purpose of the monitor (the display of up-link video) should be the controlling factor.

## REFERENCES

1. Glasford, Glenn M., Fundamentals of Television Engineering, McGraw-Hill Book Company, New York, 1955.
2. Fink, Donald G., Television Engineering Handbook, McGraw-Hill Book Company, New York, 1957.
3. Sears, Francis W., Optics, Addison-Wesley Press, Inc. Cambridge, Mass., 1949.
4. Dole, S. H., Visual Detection of Light Sources on or Near the Moon, USAF Project RAND Research Memorandum RM-1900, Santa Monica, 27 May 1957, ASTIA Document Number AD 133032
5. Parker, H. M., et. al., Evaluation of the Lunar Photometric Function, Final Report on NASA Grant NsG-468, Research Laboratories for the Engineering Sciences, University of Virginia, Charlottesville, Virginia, January 1964, Report No. AST-4015-101-64U
6. NASA Project Apollo Working Paper No. 1100, National Aeronautics and Space Administration Manned Spacecraft Center, Houston, Texas, November 22, 1963.
7. Herriman, A. G., Washburn, H. W., and Willingham, D. E., Ranger Pre-flight Science Analysis and the Lunar Photometric Model, Technical Report No. 32-384, Jet Propulsion Laboratory, Pasadena, March 11, 1963, Revised.

8. Bobrovnikoff, N. T., Natural Environment of the Moon, Technical Note 3, The Ohio State University Research Foundation, June 1959, Wright Air Development Center, Dayton, Ohio. ASTIA Document No. AD-242177.
9. Moon, Parry, The Scientific Basis of Illuminating Engineering, Dover Publications, Inc., New York, 1961.
10. Markov, A. V., The Moon, A Russian View, The University of Chicago Press, Chicago. 1960.
11. Rousculp, P. J., and W. S. Pope, Television System for a Soft-Landed Lunar Vehicle, Proceedings of National Telemetering Conference. May, 1960.
12. Newell, G. F. and W. K. E. Geddes, Tests of Three Systems of Bandwidth Compression of Television Signals, Proceedings of the I.R.E., Vol 109B, 1962. page 311.
13. Gouriet, G. G., Bandwidth Compression of a Television Signal, Proceedings of the I.R.E., Paper no. 2357R, Vol 104B, May 1957. p 265



## DISTRIBUTION

### INTERNAL

DIR  
DEP-T  
R-AERO-DIR  
    -S  
    -SP (23)  
R-ASTR-DIR  
    -A (13)  
R-P&VE-DIR  
    -A  
    -AB (15)  
    -AL (5)  
R-RP-DIR  
    -J (5)  
R-FP-DIR  
R-FP (2)  
R-QUAL-DIR  
    -J (3)  
R-COMP-DIR  
R-ME-DIR  
    -X  
R-TEST-DIR  
I-DIR  
MS-IP  
MS-IPI (8)

### EXTERNAL

NASA Headquarters  
    MTF Col. T. Evans  
    MTF Maj. E. Andrews (2)  
    MTF Mr. D. Beattie  
    R-1 Dr. James B. Edson  
    MTF William Taylor  
  
Kennedy Space Center  
    K-DF Mr. von Tiesenhausen  
  
Hayes International Corporation (5)  
    Missile and Space Support Div.  
    Apollo Logistics Support Group  
    Huntsville, Alabama

Scientific and Technical Information Facility  
P.O. Box 5700  
Bethesda, Maryland  
Attn: NASA Representative (S-AK/RKT) (2 )

Manned Spacecraft Center  
Houston, Texas  
    Mr. Gillespi, MTG  
    Miss M. A. Sullivan, RNR  
    John M. Eggleston

Donald Ellston  
Manned Lunar Exploration Investigation  
Astrogeological Branch  
USGS  
Flagstaff, Arizona